RESEARCH & DEVELOPMENT for Energy & Internal Combustion ENGINES

RD4E | INTERNAL COMBUSTION ENGINES

Multi-fuel, including Hydrogen & Ammonia based sustainable long-range Mobility

Prof. PhD. ME Victor Gheorghiu (Emeritus)

HAMBURG UNIVERSITY of APPLIED SCIENCES

Department of Mechanical Engineering & Production

https://www.victor-gheorghiu.de/

https://www.rd4e.com/

mail@victor-gheorghiu.de

grg@rd4e.com

Multi-fuel based sustainable long-range Mobility

➢ Requirements and opportunities to achieve it:

- It may be that slides 32 to 38 do not correspond to your immediate technical interests.
- If this is the case, please ignore them completely.
- If you need more detailed explanations about the content of the slides, just ask me during the video conference.

Multi-fuel based sustainable long-range Mobility

➢ Requirements and opportunities to achieve it:

- Long-range mobility requires compact, fuel-efficient, lightweight, durable, and overload-resistant drive Systems.
- For these reasons, purely electric drives such as used in BEVs, eVTOLs are not suitable.
- **Hybrid drive systems** are recommended for this purpose. These can be divided into following types:
  - Internal Combustion Engines ICE combined with Electric Motor drives and Battery storage systems EMB
  - Gas Turbines GT combined with EMB else
  - Fuel Cells FC combined with EMB.
- For military purposes, multi-fuel capability and long service life or operating time in the event of possible overloads are of crucial importance. The fuel cells FC cannot meet these requirements! The gas turbines GT are not fuel-efficient and should not be frequently overloaded. Although new developments involving the preheating of intake air through exhaust heat recovery are more efficient, they still do not match the efficiency of ICE.

See e.g. https://youtu.be/k4Rg50z7DFc?si=j2raSNC7HFbMBU0J

Multi-fuel based sustainable long-range Mobility

➢ How the VCSR ICE enables this to be achieved:

- Ultra-Downsizing (UD) concept was introduced as an even higher level of downsizing for Internal Combustion Engines ICEs. See details under SAE 2015, and SAE 2024
- The introduction of Ultra Downsizing (UD) aims to enhance the power, efficiency, and sustainability of ICEs while maintaining the thermal and mechanical strain within acceptable limits. The following approaches are utilized:

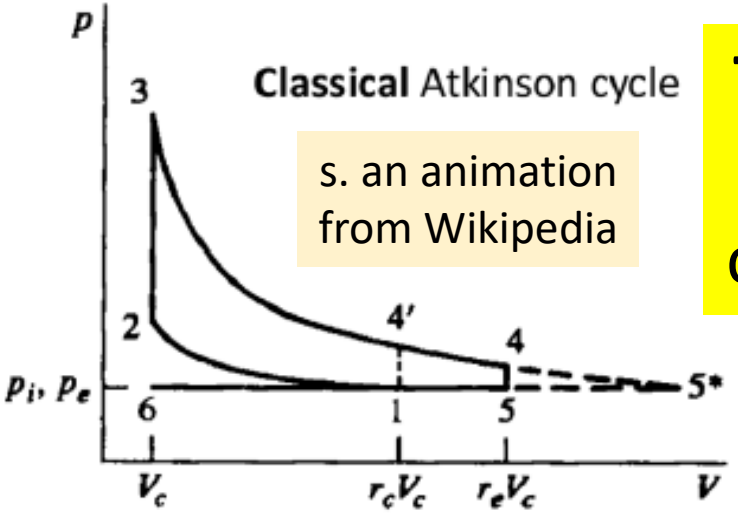
1. **True** Atkinson Cycles are implemented utilizing an asymmetrical crank mechanism called Variable Compression and Stroke Ratios (VCSR).
2. This mechanism enables shortened intake and compression and extended expansion and exhaust strokes, as well as stepless adjustment of the Volumetric Compression Ratio (VCR).
3. Unrestricted two or more stage high-pressure turbocharging and intensive intercooling: This setup enables more complete filling of the cylinder and reduces the compression work on the piston, resulting in higher specific power and efficiency.
4. The new Load Control (LC) approach is based to continuous VCR adjustment.

Multi-fuel based sustainable long-range Mobility

➢ How the VCSR ICE enables this to be achieved:

5. By adjusting the VCR without resorting to excessive throttling or external Exhaust Gas Recirculation (EGR), a stoichiometric Air Fuel Ratio (AFR) can be maintained. This facilitates easier exhaust gas aftertreatment (if desired) using a three-way catalyst.
6. Fuel Flexibility: The continuous VCR adaptation capability enables the engine to operate in multi-fuel mode. In addition to gasoline or diesel, the engine can also run on alternative fuels like pure hydrogen (H_2) or H_2 blended with gases like CNG, Biogas, e-fuels, or even ammonia (NH_3). This versatility allows for reduced carbon emissions and increased sustainability.
7. By combining these approaches, the UD concept aims to achieve higher power output, improved efficiency, and reduced environmental impact in ICEs, all while ensuring the durability and strength of engine components remain within acceptable limits.

Thermodynamics
Introduction
continuation S. 23



Classical Atkinson cycle

s. an animation from Wikipedia

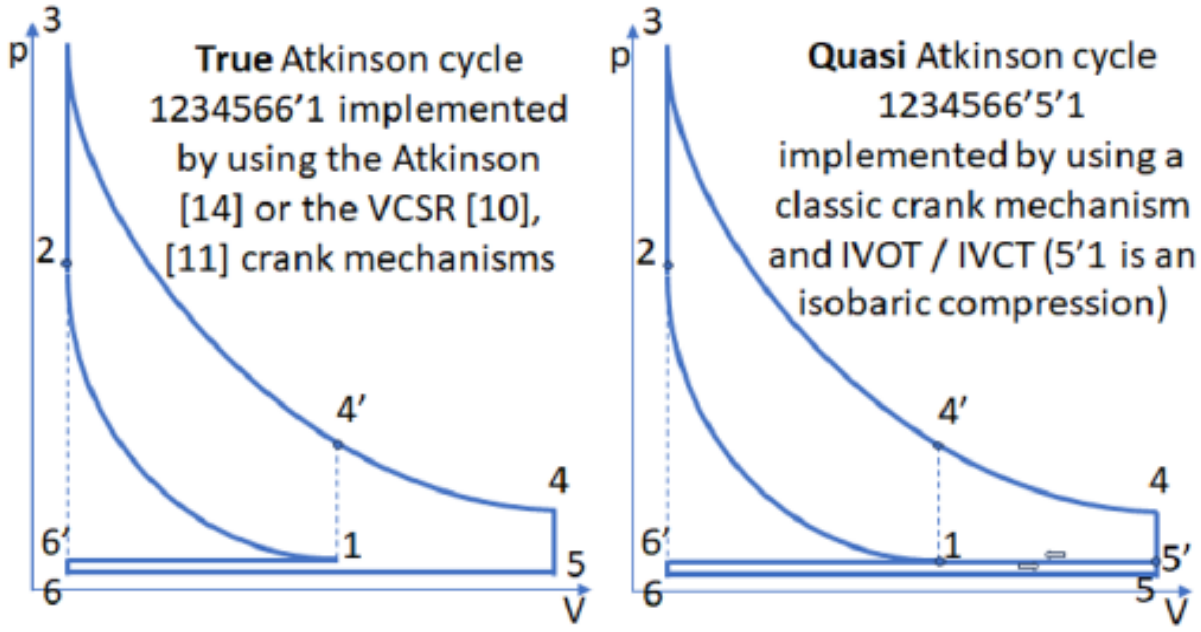


Fig. 1 / page 2 of SAE 2024-01-2096

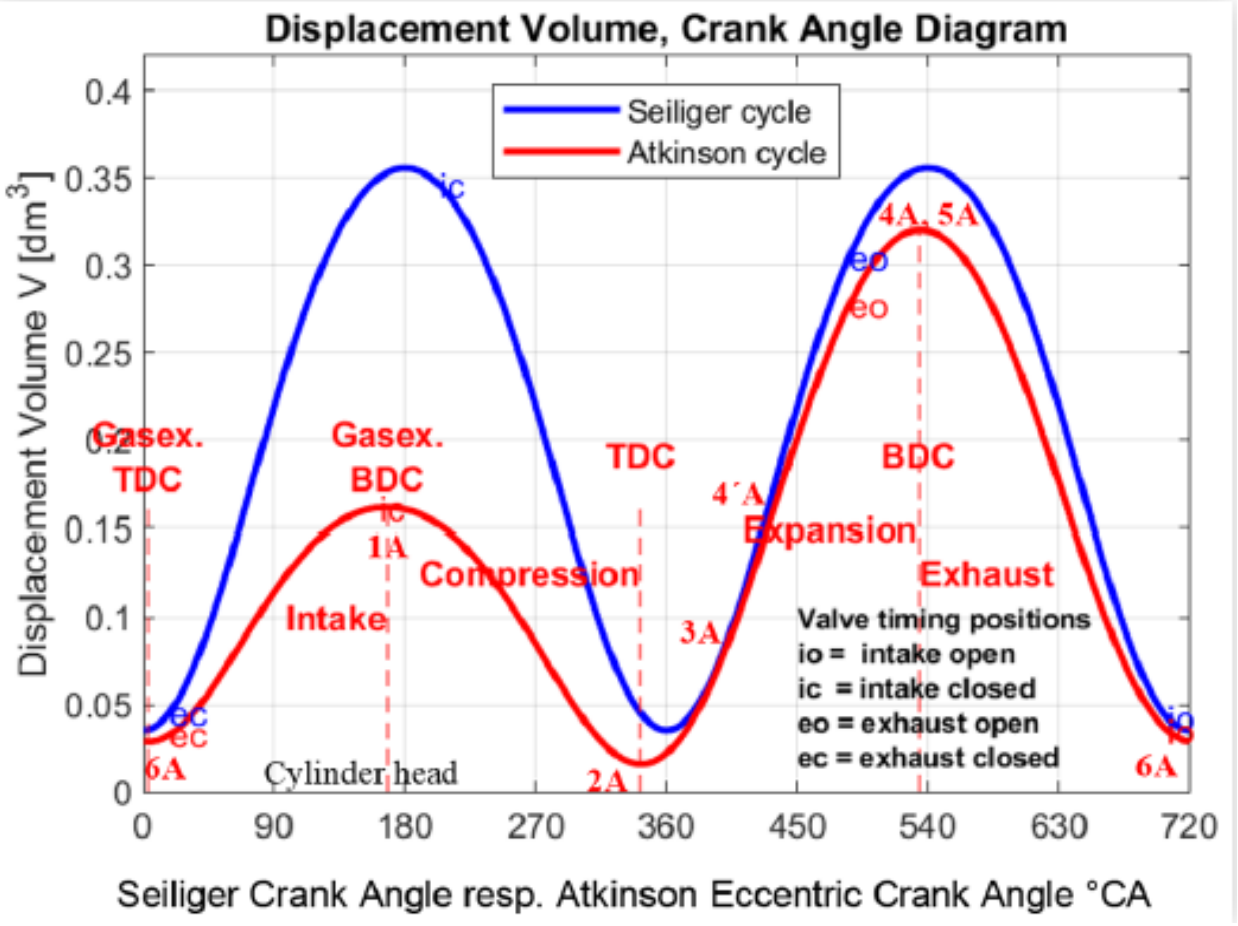


Fig. 4 / page 5 of SAE 2024-01-2096

Seiliger cycle generally refers to Otto- and Diesel cycles

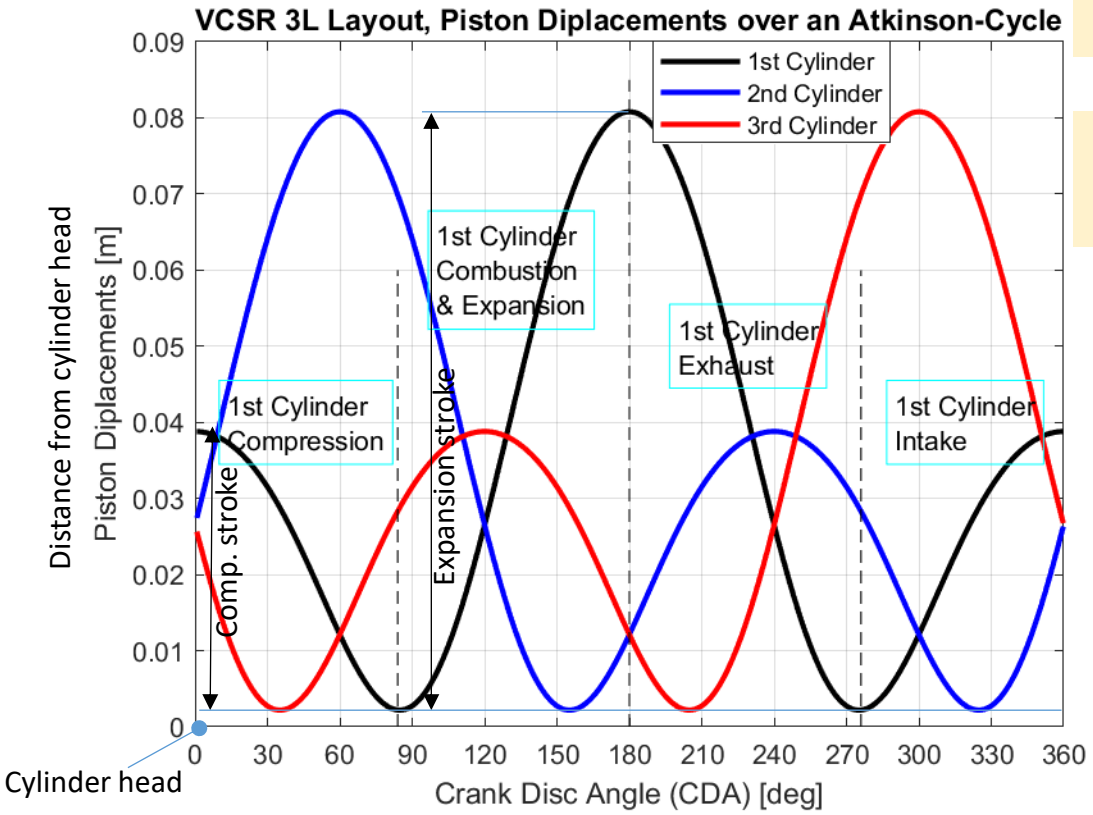
True Atkinson cycle consists of the following processes:

6'-1 Intake into Cylinder	4-5 Exhaust & Expan. in Turbine
1-2 Compression in Cylinder	5-6 Intake in Compressor
2-3 Combustion in Cylinder	6-6' Compression in Compressor
3-4 Expansion in Cylinder	

VCSR means Variable Compression and Stroke Ratios

Crank mech. kinetics

Animations of VCSR crank mechanism in two Principle Design Variants **PDV** & cylinder arrangements:



Click on icons > to play videos

2nd PDV for VCR: low, mean & high

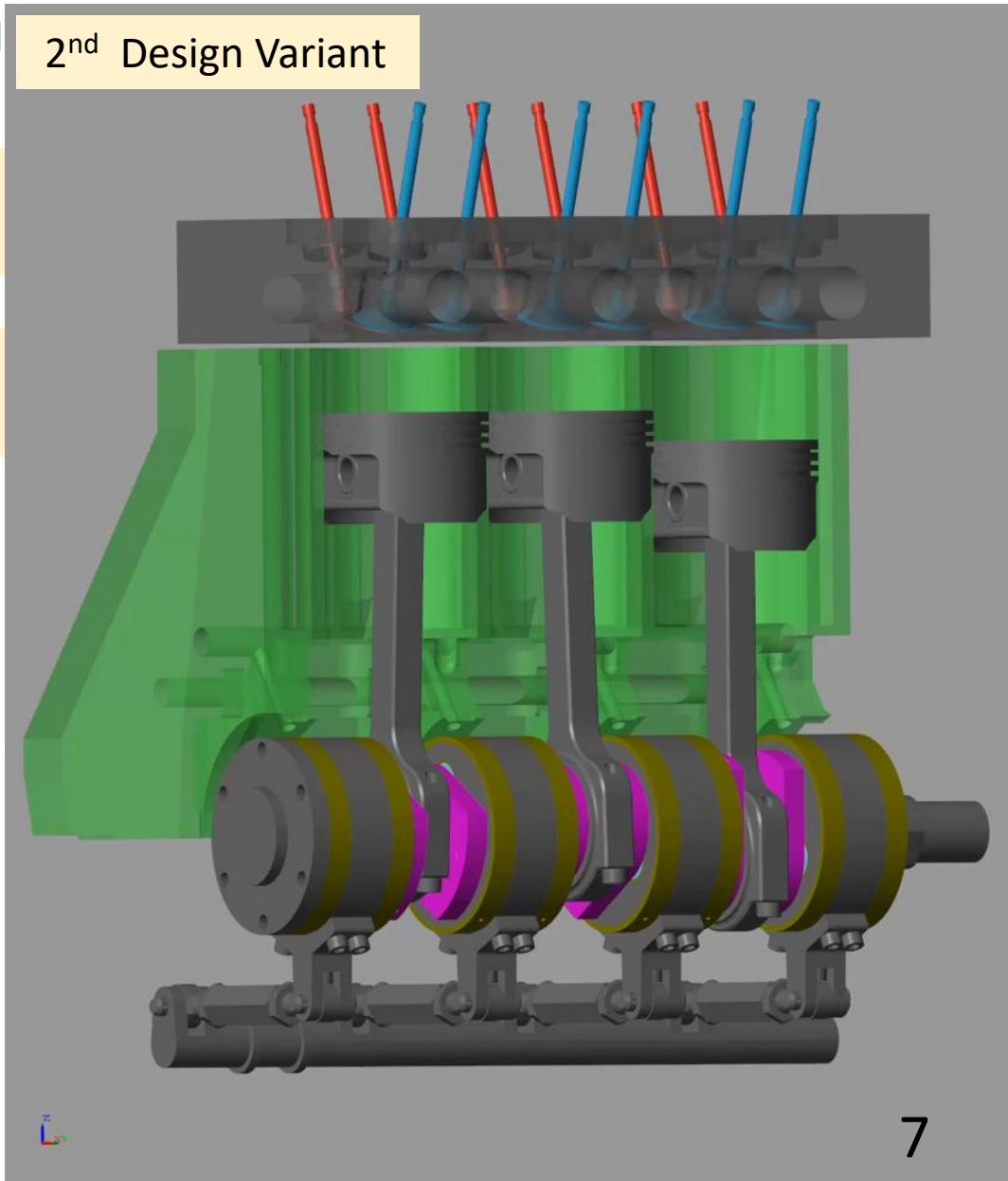
1st PDV for VCR: low, mean & high

Due to the variable Volumetric Compression Ratio VCR, shortened compression & extended expansion strokes, the efficiency of the VCSR ICE is between 25 and 45 % higher than by the classic ICE.

➢ [Paper2015], [Pres2019], [Paper2021], [Paper20224]

Note the very low connecting rod angle inclination during high-pressure processes! This reduces the usual limits of the normal force of the piston on the cylinder walls.

3L - Cylinders arrangements, only exterior view



Appendix 3. Short Presentation and Comments of the first two of five Principle Design Variants PDV from the granted patents [10] and [11]:

Table A3-1, Components Designation in all VCSR crankshaft drive variants, i.e. of VCSR basic working principle BWP Variants, and other Notations

Nr.	Reference meaning for all five PDVs	Nr.	Reference meaning for all five PDVs
1	Cylinder axis	13	Eye of the ring gear lever for adjusting the VCR
2	Shaft axis	14	Counter weight
3	Crankpin and eccentric shaft axis are identical	15	Crankcase
4	Eccentric pin axis	16	Piston
5	Shaft journal	17	Piston pin
6	Crank cheek	18	Rolling bearing (needle bearing)
7	Half crank pin resp. eccentric shaft	19	Connecting road
8	Eccentric cheek piece	20	Cylinder
9	Eccentric crankpin	21	So-called connecting rod fiddle, i.e. the area covered by all crank mechanism extremities during its turning over, s. here
10	Planetary gear of the eccentric	22	Minimum diameter of the crankcase
11	Ring gear	23	Locating curve of the eccentric pin (thus the axis of the big connecting rod eye)
12	Sun gear		

The VCSR in Variant 1 of the PDV, (originally referred to as variant **HR_PSR_intern_2U** in [10] and [11]), is shown in the original Figs. 1 through 4.

The transmission ratio and the synchronization between the gears (10) and (11) of the planetary gear to create the necessary four piston strokes of the four-stroke true Atkinson process are selected in such a way as to force only one rotation of the planet gears (10) after two crankshaft rotations (2U) so that the ratio between the planet gears (10) and ring gears (11) must be 2:3.

For synchronization purposes of the two cranks, the eccentric crank cheek (8) and pin (9) must be directed perpendicularly to the crank cheek (6) and crankpin (3) when (6) and (3) are directed towards TDC and the lever eyes (13) are in the zero position (as in Fig. 1 and right cylinder from Fig 2).

Gearing ratio verification for Variant 1 of VCSR crank mechanism from [10] and [11] according to the Theory of Planetary Gears from Appendix 4.

Specified parameters and exemplary dimensions:

Parameters of Variant 1 according to the theory of Planetary Gears from **Appendix 4**

$\omega_C := 2 \qquad \omega_P := -1 \qquad \omega_R := 0$

Exemplary dimensions

$r_P := 0.06\,m$

PDV Variant 1

Results and Comments, from equation (7k) it results

$$g_{RP} := \frac{\omega_C - \omega_P}{\omega_C} \qquad g_{RP} = 1.5 \qquad \frac{1}{g_{RP}} = \frac{2}{3} \qquad (7k)$$

$r_R := r_P \cdot g_{RP} \qquad r_R = 0.09\,m$

i.e. according to (3g) no Sun is present!

An animation of this VCSR crank mechanism Variant 1, according to the original Figures 1 through 4, is presented here.

More animations of the kinematic of Variant 1 in 3Y cylinder arrangement are presented here for three Values of the VCR: low, mean and high.

The lower values of connecting rod inclination during the combustion and expansion "burn & exp area" parts of the true Atkinson cycle are especially noteworthy. These produce lower values of the piston side forces and thus of the piston/cylinder friction.

Appendix 4. Theory of Planetary gears, according to the Help of Matlab / Simulink / Simstate / Driveline / Gears

A complete Planetary Gear (PG) usually consists of the following components: sun (S), one or many planets (P), carrier (C) and ring gear (R).

It is possible that one of these components may be missing in some configurations or may not be present due to existing geometric constraints.

A planetary gear has the following parameters:

r_C	is the radius of the Carrier gear.	ω_C	is the angular velocity of the Carrier gear.
r_S	is the radius of the Sun gear.	ω_S	is the angular velocity of the Sun gear.
r_P	is the radius of the Planet gear.	ω_P	is the angular velocity of the Planet gear.
r_R	is the radius of the Ring gear.	ω_R	is the angular velocity of the Ring gear.
g_{XY}	are the gear ratios of the (X,Y) gear pairs	τ_x	ist the torque transfer for the x gear.

A Planetary Gear imposes some kinematik (k) and geometric (g) constrains:

$r_C \cdot \omega_C = r_S \cdot \omega_S + r_P \cdot \omega_P \qquad (1k)$

$r_R \cdot \omega_R = r_C \cdot \omega_C + r_P \cdot \omega_P \qquad (2k)$

$$g_{RS} = \frac{r_R}{r_S} = \frac{N_R}{N_S} > 1 \qquad (3k)$$

$$g_{RP} = \frac{r_R}{r_P} = \frac{N_R}{N_P} > 1 \qquad (4k)$$

$$g_{PS} = \frac{r_P}{r_S} = \frac{N_P}{N_S} > 1 \qquad (5k)$$

$r_C = r_S + r_P \qquad (1g)$

$r_R = r_C + r_P = r_S + 2 \cdot r_P \qquad (2g)$

Condition for the presence of the sun in PG: $r_S > 0$ according to (2g) $r_R > 2 \cdot r_P$ and to (4k) $g_{RP} > 2 \qquad (3g)$

In terms of ratio (3k), the key kinematic constrain is:

$(1 + g_{RS}) \cdot \omega_C = \omega_S + g_{RS} \cdot \omega_R \qquad (6k)$

The four degrees of freedom for Ring-Sun (R,S) gear pair reduce to two independent degrees of freedom. The gear pairs are (S,P) and (P,R).
The torque transfer is

$g_{RS} \cdot \tau_S + \tau_R - \tau_{loss} = 0$ In the ideal case where is no torque loss, that is $\tau_{loss} = 0$

In terms of ratio (4k), the key kinematic constrain is:

$g_{RP} \cdot \omega_R = \omega_P + (g_{RP} - 1) \cdot \omega_C \qquad (7k)$

The three degrees of freedom for Ring-Planet (R,P) reduce to two independent degrees of freedom. The gear pair is (P,R).
The torque transfer is

$g_{RP} \cdot \tau_P + \tau_R - \tau_{loss} = 0$ In the ideal case where is no torque loss, that is $\tau_{loss} = 0$

In terms of ratio (5k), the key kinematic constrain is:

$\omega_S = -g_{PS} \cdot \omega_P + (1 + g_{PS}) \cdot \omega_C \qquad (8k)$

The three degrees of freedom for Sun-Planet (S,P) reduce to two independent degrees of freedom. The gear pair is (S,P).
The torque transfer is

$g_{PS} \cdot \tau_S + \tau_P - \tau_{loss} = 0$ In the ideal case where is no torque loss, that is $\tau_{loss} = 0$

PDV Variant 1

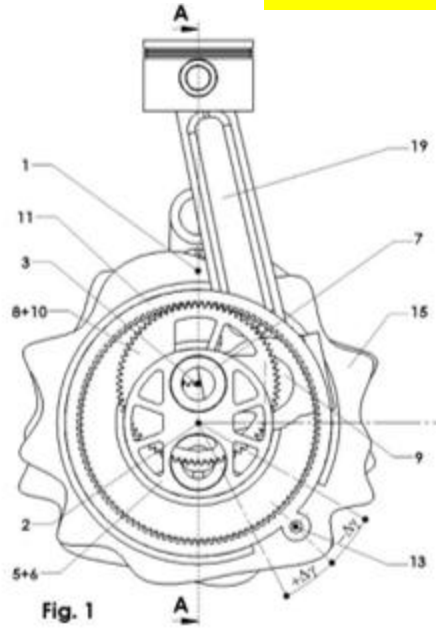


Fig. 1

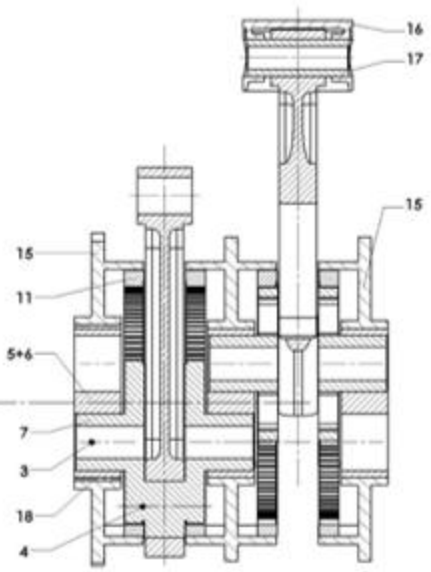


Fig. 2

Nr.	Reference meaning for all five PDVs
13	Eye of the ring gear lever for adjusting the VCR
14	Counter weight
15	Crankcase
16	Piston
17	Piston pin
18	Rolling bearing (needle bearing)
19	Connecting rod
20	Cylinder
21	So-called connecting rod fiddle, i.e. the area covered by all crank mechanism extremities during its turning over, s. here
22	Minimum diameter of the crankcase
23	Locating curve of the eccentric pin (thus the axis of the big connecting rod eye)

Nr.	Reference meaning for all five PDVs
1	Cylinder axis
2	Shaft axis
3	Crankpin and eccentric shaft axis are identical
4	Eccentric pin axis
5	Shaft journal
6	Crank cheek
7	Half crank pin resp. eccentric shaft
8	Eccentric cheek piece
9	Eccentric crankpin
10	Planetary gear of the eccentric
11	Ring gear
12	Sun gear

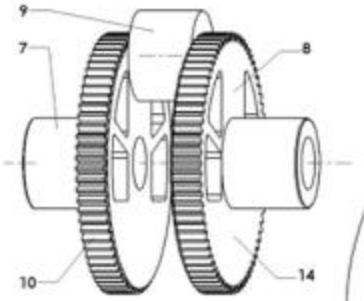


Fig. 3

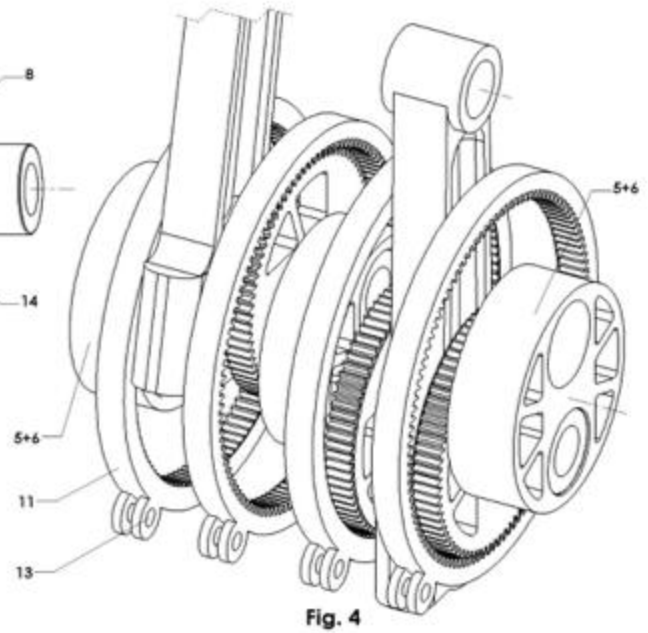


Fig. 4

Figure A3-V1, View and section of the VCSR in Variant 1. Fig. 3 shows the eccentric crank with its eccentric gears.

The **VCSR in Variant 2 of the Principle Design Variant PDV**, (originally referred to as variant HR_PSR_*_1U in [10] and [11], where * can be one of "internal", "external", "mixed"), is shown in the original Figs. 5 through 7.

The transmission ratio and the synchronization between the gears (10) and (11) of the planetary gear to create the necessary four piston strokes of the four-stroke true Atkinson process are selected in such a way as to force only two rotations of the planet gears (10) after one crankshaft rotation (1U) so that the ratio between the planet gears (10) and ring gears (11) must be 1:3. For the synchronization purposes of the two cranks, the eccentric crank (s. Fig. 7) cheek (8) and pin (9) must be directed against to the crank cheek (6) and crankpin (3) when (6) and (3) are directed towards TDC (s. left cylinder in Fig. 6 & 5) and the lever eyes (13) are in the zero position (as in Fig. 5).

Gearing ratio verification for Variant 2 of VCSR crank mechanism from [10] and [11] according to the Theory of Planetary Gears from Appendix 4.

Parameters of Variant 2 according to the theory of Planetary Gears from **Appendix 4**

$\omega_C := 1 \qquad \omega_P := -2 \qquad \omega_R := 0$

Exemplary dimensions

$r_P := 0.02\ m$

Results and Comments, from equation (7k) it results

$$g_{RP} := \frac{\omega_C - \omega_P}{\omega_C} \qquad g_{RP} = 3 \qquad \frac{1}{g_{RP}} = \frac{1}{3} \qquad (7k)$$

$r_R := r_P \cdot g_{RP} \qquad r_R = 0.06\ m \qquad (4k)$

$r_S := r_R - 2 \cdot r_P \qquad r_S = 0.02\ m \qquad (2g)$

$$g_{PS} := \frac{r_P}{r_S} \qquad g_{PS} = 1 \qquad (5k)$$

$$\omega_S := -g_{PS} \cdot \omega_P + (1 + g_{PS}) \cdot \omega_C \qquad \omega_S = 4 \qquad (8k)$$

An animation of this VCSR crank mechanism Variant 2, according to the original Figures 5 through 7, is presented here and a VCR variation here.

More animations of the kinematic of Variant 2 in 3Y cylinder arrangement are presented here for three Values of the VCR: low, mean and high.

The **lower values of connecting rod inclination during the combustion and expansion** "burn & exp area" parts of the true Atkinson cycle are especially noteworthy. These produce lower values of the piston side forces and thus of the piston/cylinder friction.

PDV Variant 2

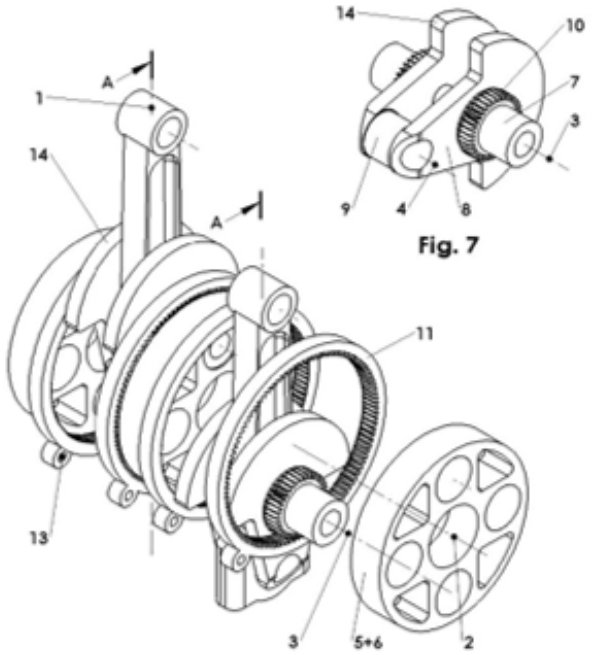


Fig. 5

Fig. 7

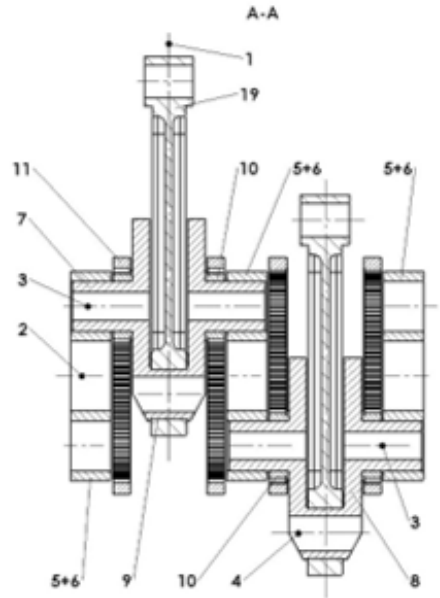


Fig. 6

Figure A3-V2, View and section of the VCSR in Variant 2. Fig. 7 shows the eccentric crank with adjacent (referred to as "internal" sub-variant) eccentric gears.

Appendix 5. Sim. model for a cylinder of both the Classic and the VCSR ICE in PDV Variant 2

Simscape/Multibody simulation model of cylinder 1 of the classic ICE is presented in Fig. A5-1. Input < 2 > at VCSR is linked to the EC crank.

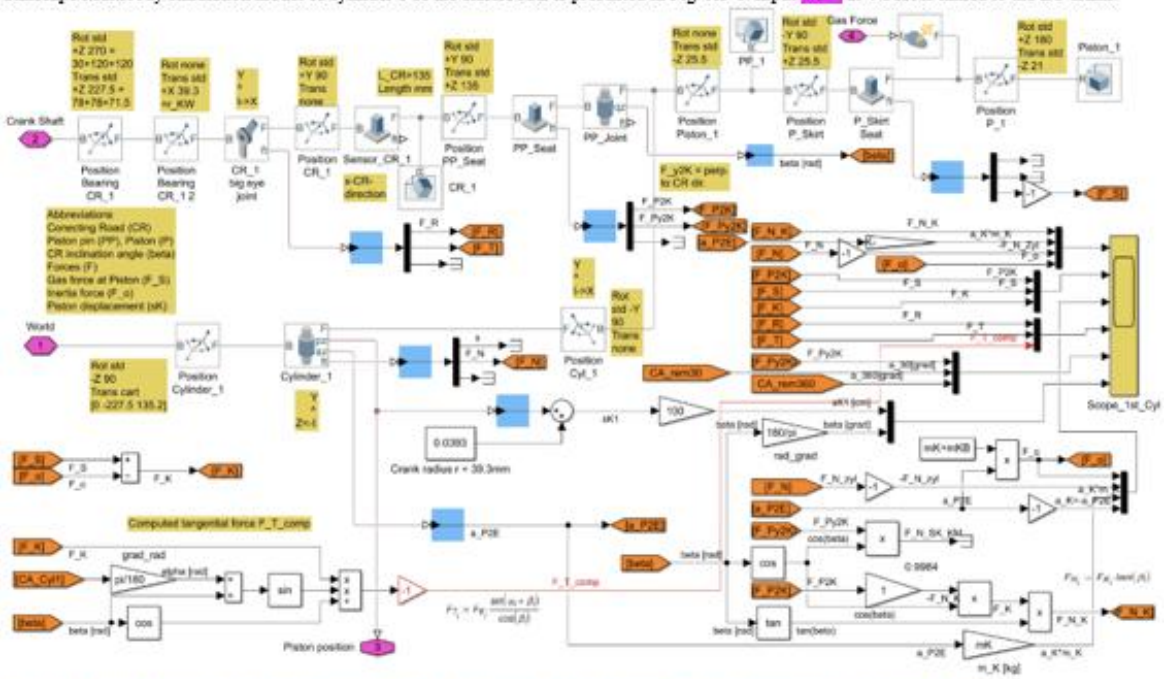


Fig. A5-1, Simulink/Simscape/Multibody Model of Cylinder 1. The Simulation Results of Scope_1st_Cyl are presented in Fig. A1-3 and A1-4.

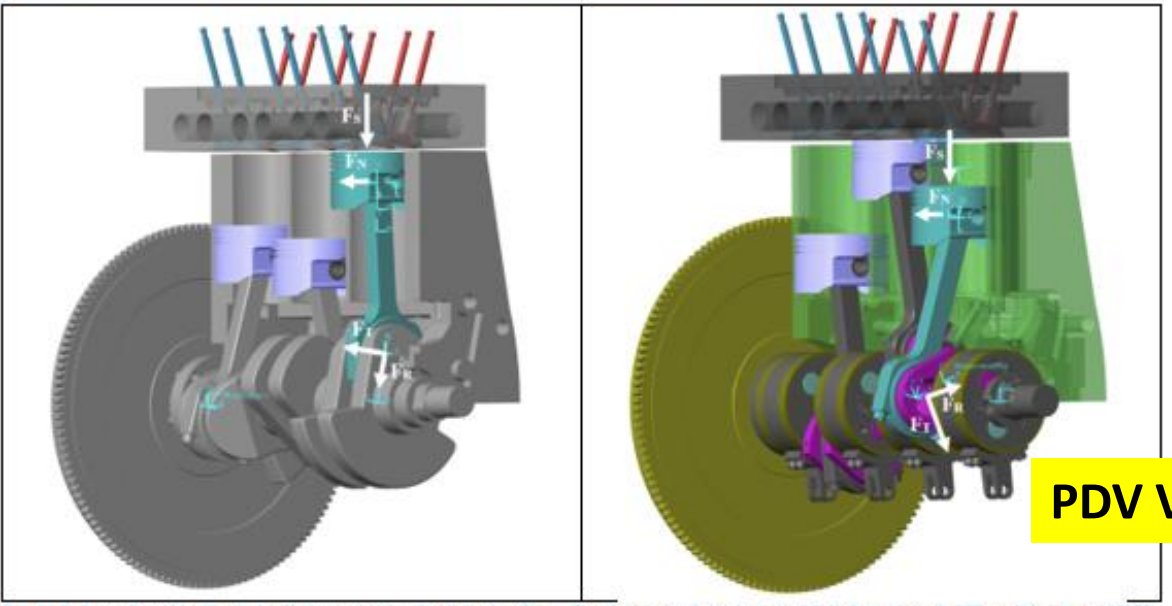


Fig. A5-2, Screenshot of the Mechanics Explorers showing the alignment of some Forces of the crank mechanism of Cylinder 1 of classic ICE (on left side) and VCSR ICE (on the right side). F_S is the Gas Force acting on the Piston. F_T and F_R are the tangential and radial forces acting on the crankpin (on left side) and on the eccentric crank (on right side), respectively. F_N is the normal force from piston to the cylinder wall.

Forces and Kinematic

Simulation Results for **classical (working according to Seiliger cycle) ICE**. 1st Cylinder in Engine Operating Point EOP 15 s. Fig A5-3. The thermodynamic behavior in this EOP is depicted in SAE_2024-01-2096, Figure A2-EOP-15 of Appendix 2. The pressure from this Seiliger cycle produces the gas force F_S. The normal force to cylinder wall -F_N = F_N_Zyl is computed by Simscape and checked by means of the known formula by F_N_K, where "alpha" is the crank angle CA and "beta" the inclination angle of the connecting rod. F_o is the inertia force produced from the oscillating masses (piston, piston pin, piston rings and a part of the connecting rod). Piston mass m_K accelerates at a_K produces the red curve of inertia force.

F_P2K is the force induced from piston on connecting rod x-axis. F_K is the resulting force of F_S and F_o. a_K is the piston acceleration on cylinder axis. F_R and F_T are presented as F_R and F_T in Fig. A5-2. F_Py2K is the force induced from piston on the connecting rod y-axis (i.e. cross to x-axis). In order to establish a correlation with the crank angle CA, the residuals of CA divided by 30 resp. 360, i.e. a_30 and a_360 (a crank rotation) are plotted. sK1 is the piston displacement and beta is the inclination angle of the connecting rod.

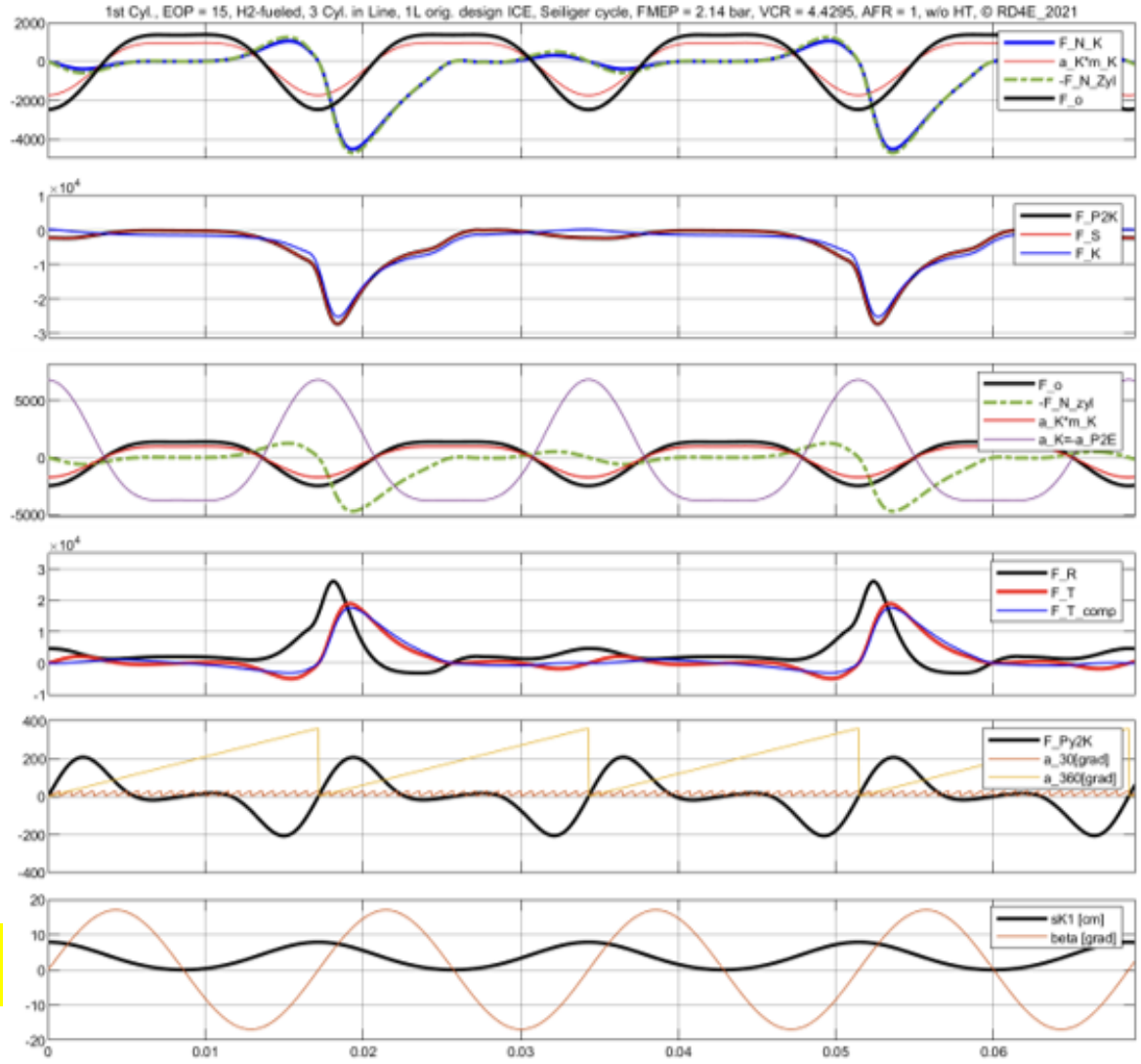


Fig. A5-3, Simulation results along two engine cycles from the Scope_1st_Cyl over the time in seconds for classical (**working according to Seiliger cycle**) ICE in Engine Operating Point EOP 15. All forces are in Newton. The cylinder pressure is the same to that of in SAE_2024-01-2096, Appendix 2, Fig. A2-EOP-15.

Appendix 6. Simulation results for some Forces and Torques from VCSR ICE crank mechanism in Basic PDV Variant 2, Layout 3L (i.e. 3 cylinder in line) in Engine Operation Point EOP 15.

The simulation are done by Matlab/Simulink/Simscape/Multibody tools. Deformations of all engine components as a result of the mechanical loads are not considered here, i.e. the components are not deformable. In addition, no frictions between these components are taken into account.

Forces exemplary

Study of PDV Variant 2, for layout 3L

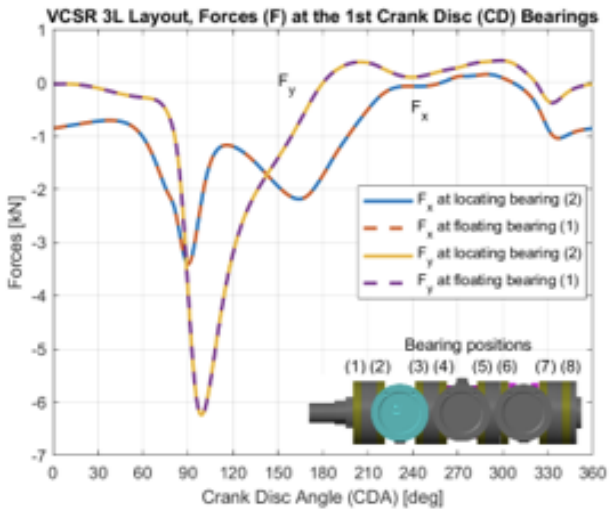


Figure A6-1, Forces in Bearings 1 and 2 of the 1st CD.

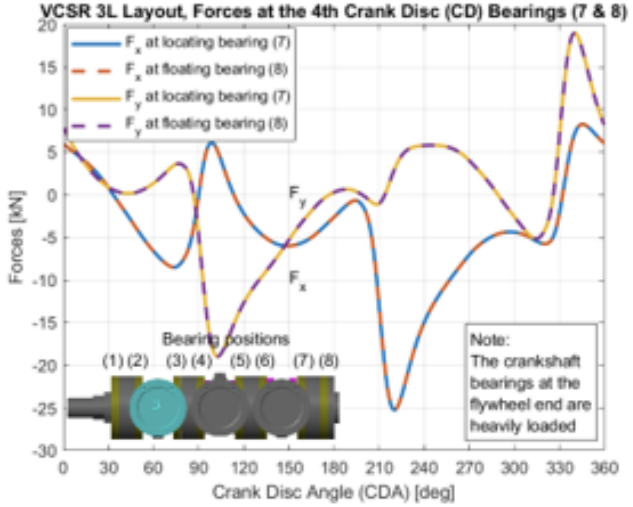


Figure A6-2, Forces in Bearings 7 and 8 of the 4th CD produce by eccentric E3 in PG4.

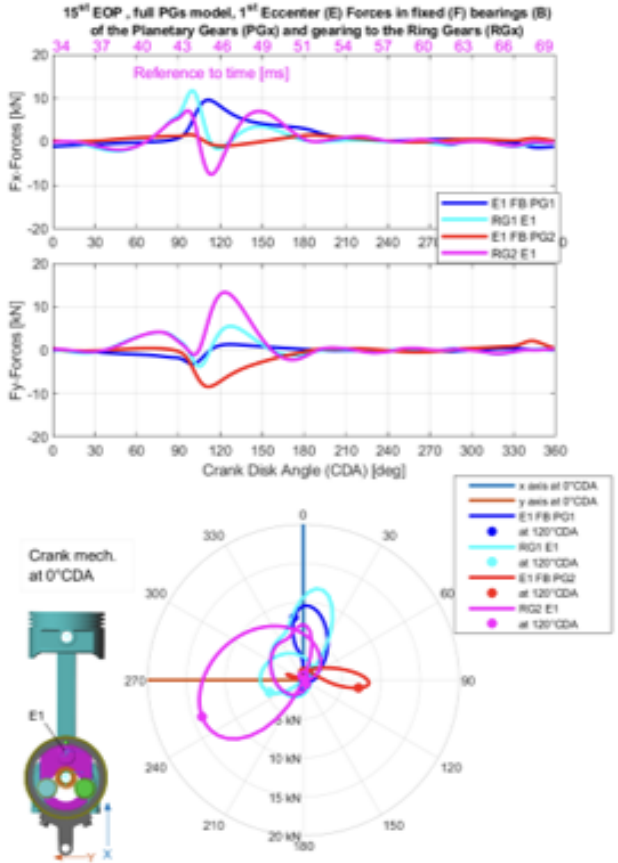


Figure A6-3, Forces produced by Eccentric E1 in its bearings (E1 FB) in the PG1 and PG2 and in its gearings with RG1 and RG2 (RG1 E1, RG2 E1). In Figs 3-1, 3-2 and 3-3 are shown detail views of this crank mechanism part. In the upper half of this figure, an additional time axis is introduced in magenta at the top to allow the correlation with the curves from figure A5-4 from the Appendix 5.

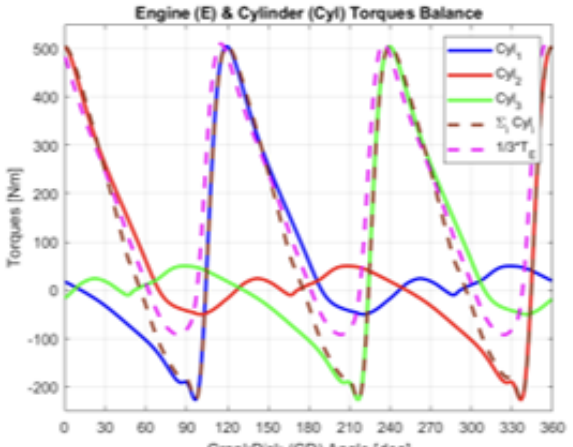


Figure A6-4, Engine and Cylinder torques balances in 15st EOP, 3L VCSR. T_g is the induced torque at engine crankcase, it is divided by 3 because of the 1/3 gear ratio in the PGs. The cylinder torques are at the eccentric cranks EC_i, i.e. the product between the tangential force F_Y and the eccentric crank length "e", where i = 1.2.3. The Σ_i Cyl$_i$ is the sum of these three cylinder torques. The deviation between the Σ_i Cyl$_i$ and 1/3*T_g is caused by the inertia of the crank mechanism components.

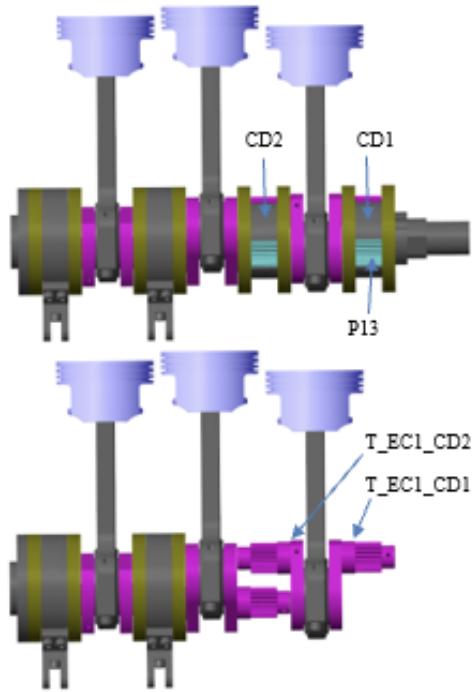
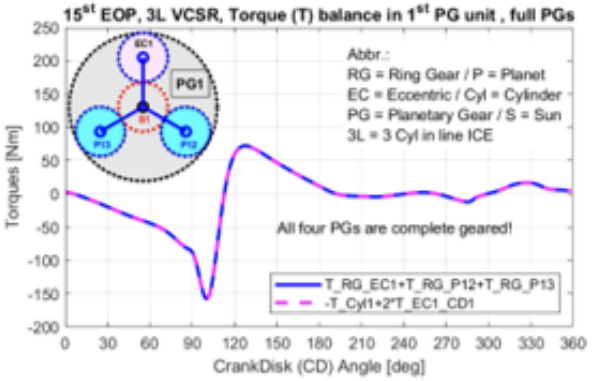


Figure A6-5 auxiliary. Explanation pictures to Fig. A6-5

PDV Variant 2, 3L



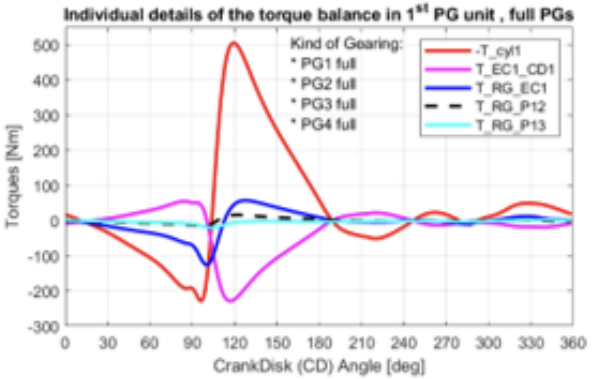
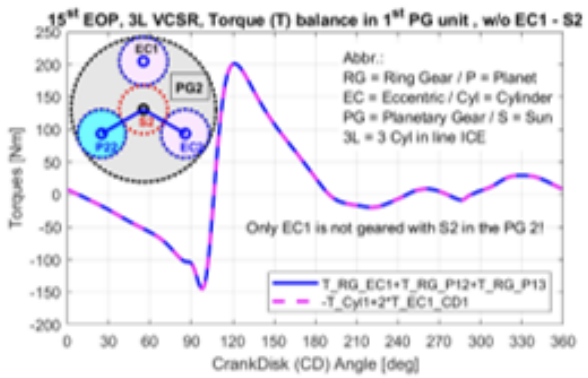


Figure A6-5, Torque balance in 1st PG in the layout case, where all PGs are completely geared (full), i.e. its eccentric planets, sums and planets are geared. The toothed gear pairs are shown by the connecting lines in the top left picture. The verification of the torque balance in PG1 is shown in the upper part of the figure.

T_RG_EC1, T_RG_P12, T_RG_P13 are the torques that are exchanged between the eccentric EC1, the planets P12, P13 and the ring gear respectively.

T_EC1_CD1 is the torque part of T_Cyl1 transferred to the crank disc 1 i.e. CD1. In the Simscape model of the eccentric crank, the torque T_EC1_CD2 is twice as large as T_EC1_CD1.

Torques exemplified with different toothing in PG2 and full toothing of the other PGs



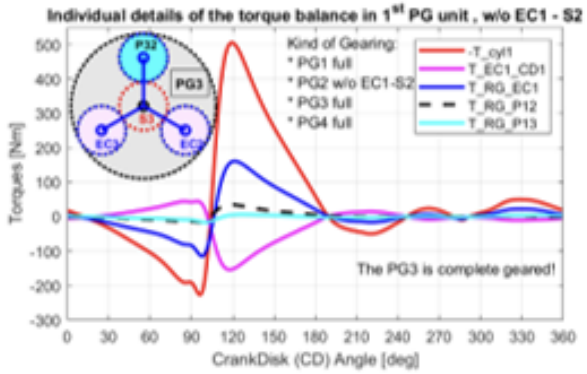
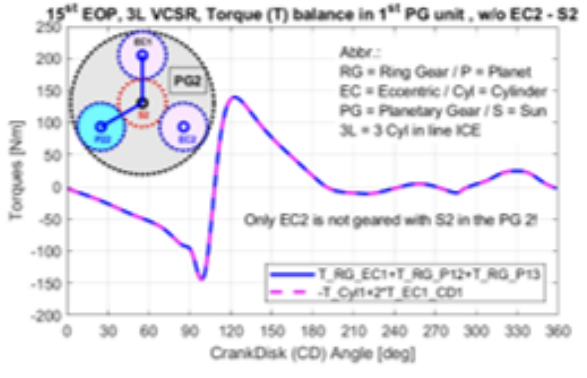


Figure A6-6, Torque balance in 1st PG in the layout case, where, except PG2, all other PGs are completely geared (full), i.e. its eccentric planets, suns and planets are geared. The toothed gear pairs are shown by the connecting lines in the top left picture. The eccentric EC1as shown in PG2 is not geared to the sun S2. The verification of the torque balance in PG1 is shown in the upper part and the individual torques are in the lower part of the figure.



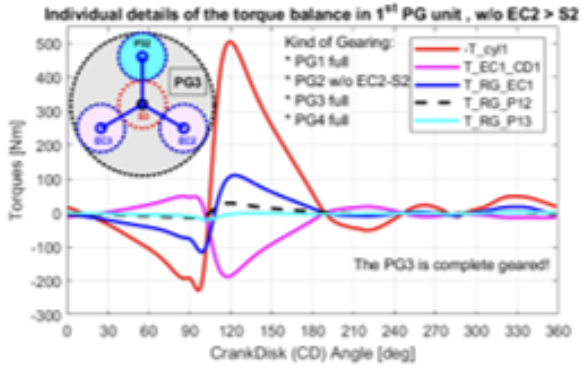
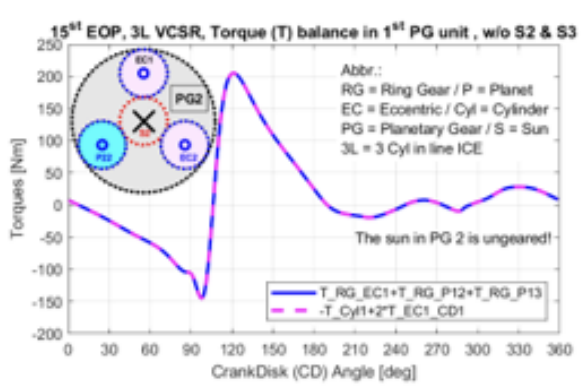


Figure A6-7, Torque balance in 1st PG in the layout case, where, except PG2, all other PGs are completely geared (full), i.e. its eccentric planets, suns and planets are geared. The toothed gear pairs are shown by the connecting lines in the top left picture. The eccentric EC2 as shown in PG2 is not geared to the sun S2. The verification of the torque balance in PG1 is shown in the upper part and the individual torques are in the lower part of the figure.

Torques exemplified with more different toothing in PGs



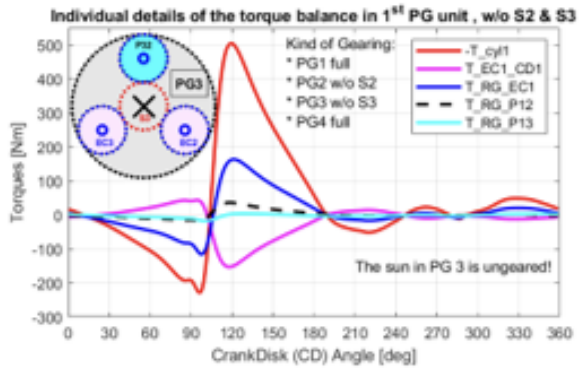
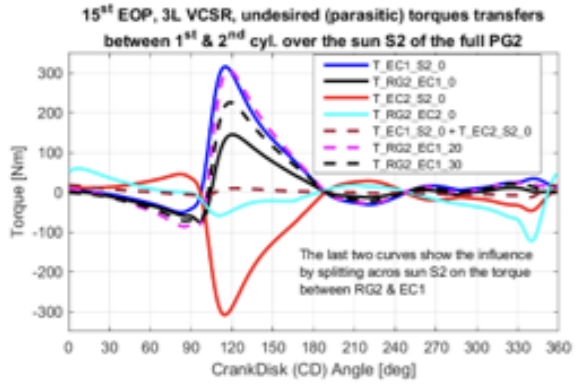


Figure A6-8, Torque balance in 1st PG in the layout case, that the suns S2 and S3 in PG2 resp. PG3 are ungeared with the eccentrics and planets. The verification of the torque balance in PG1 is shown in the upper part and the individual torques are in the lower part of the figure.



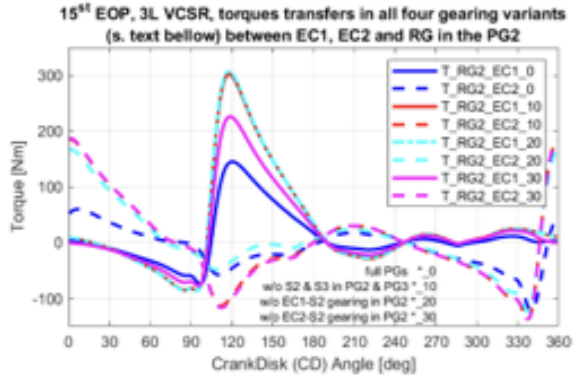


Figure A6-9, Torques balance in 1st PG in four layout cases. The gearing in these cases are indicated in the text from lower part of the figure. The respective torques can be recognized by the suffixes "xx" of their names. The variant discussed in the Fig. A6-8, for example, has the suffix "10". In the upper part of the figure, the torques T_EC1_S2_0 and T_EC2_S2_0 act on the sun against each other, i.e. parasitically in the full toothed PG2.

The different torques transferred from EC1 to RG1 and CD1 shown in Figures. A6-5 to A6-7 indicate that parasitic torques are exchanged between EC1 and EC2 in PG2. This applies to all other fully toothed PGs.

An additional presentation of the parasitic torques is done in the Fig. A6-9 for four gearing variants in PGs.

This applies to all other fully toothed PGs that are located between cylinders or cylinder groups.

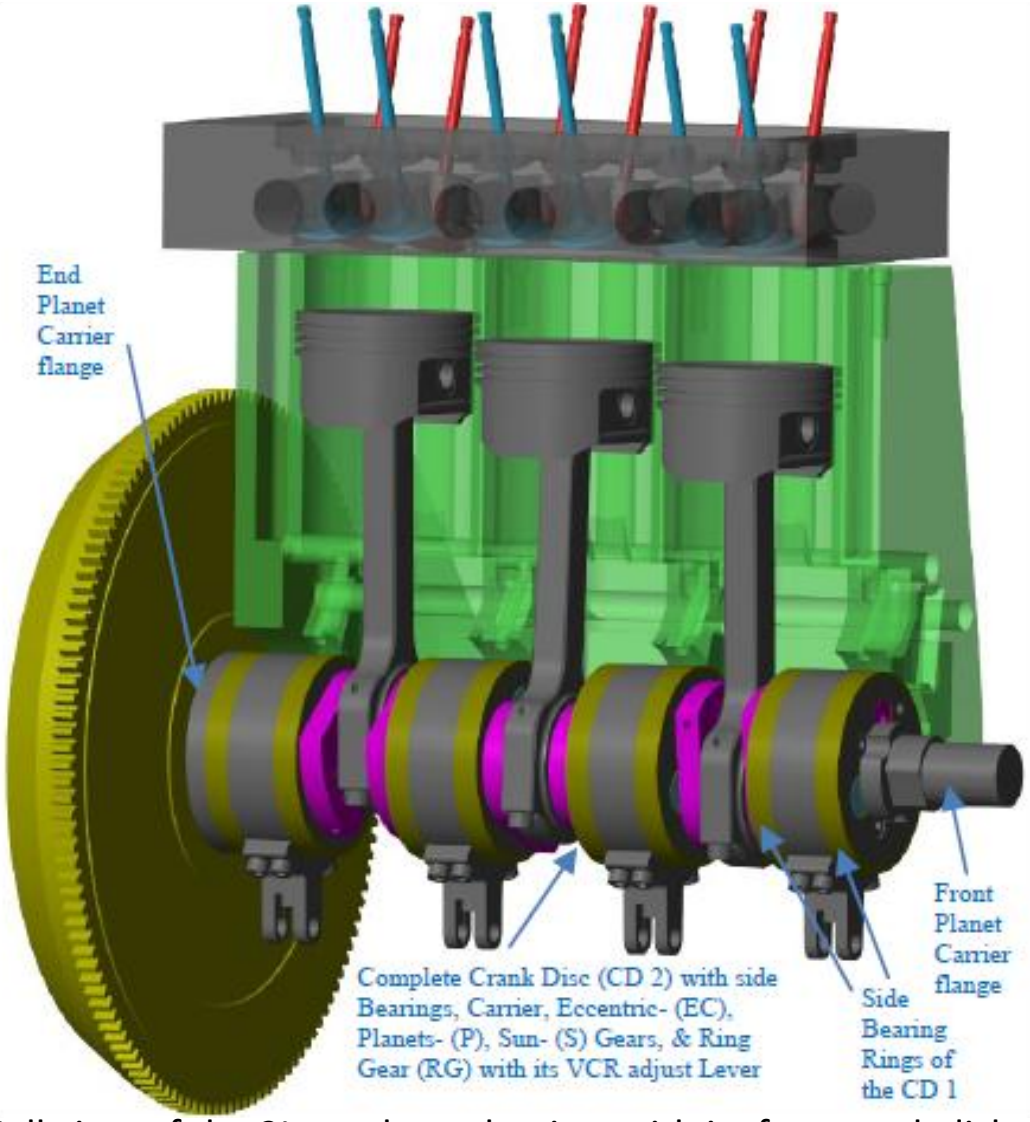
There are two simple ways to avoid this:

a) Either one designs the three cylinders in a 3Y arrangement, i.e. without PGs between the cylinders.

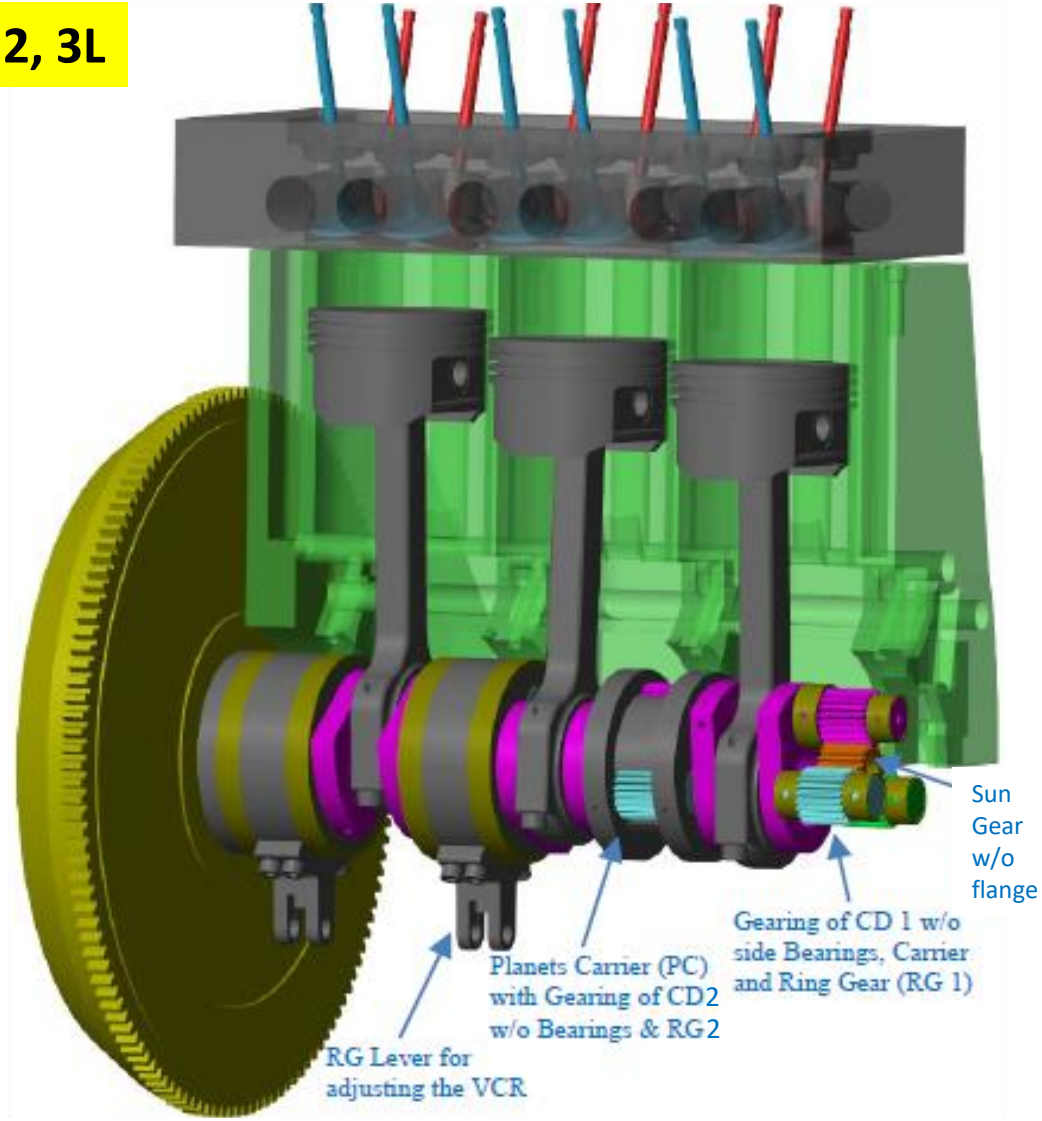
b) Or one doubles the fully toothed PGs between the cylinders or cylinder groups and connects them via their carriers. Thus, each sun is interlocked with only one eccentric planet. This additionally enables the setting of different VCR values in each cylinder or group of cylinders and even a thermodynamic cylinder deactivation according to claim 9 of the patents [10], [11].

PDV Variant 2, 3L

PDV Variant 2, 3L

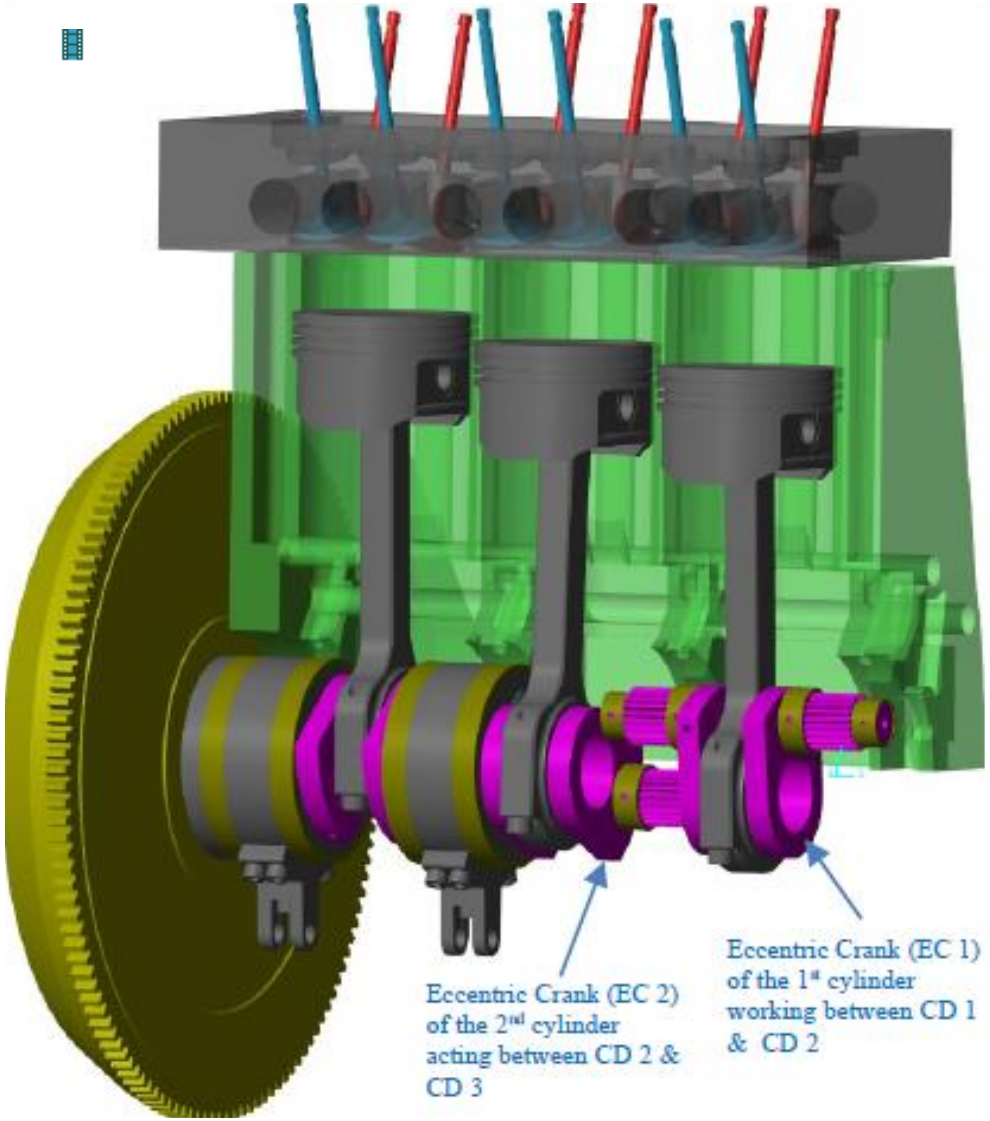


Full view of the 3L crank mechanism with its four crank disks (CD), their Slide- or Roll-bearing Rings and VCR adjust levers connected at each Ring Gears (RG), crl+clik for animations of this crank mechanism. The CDs act as shaft journals. Because the CDs have the half rotation speed of the eccentric cranks (EC) - like the camshaft of a classical engine – CDs can also carry the cams for valve actuating (not shown here).

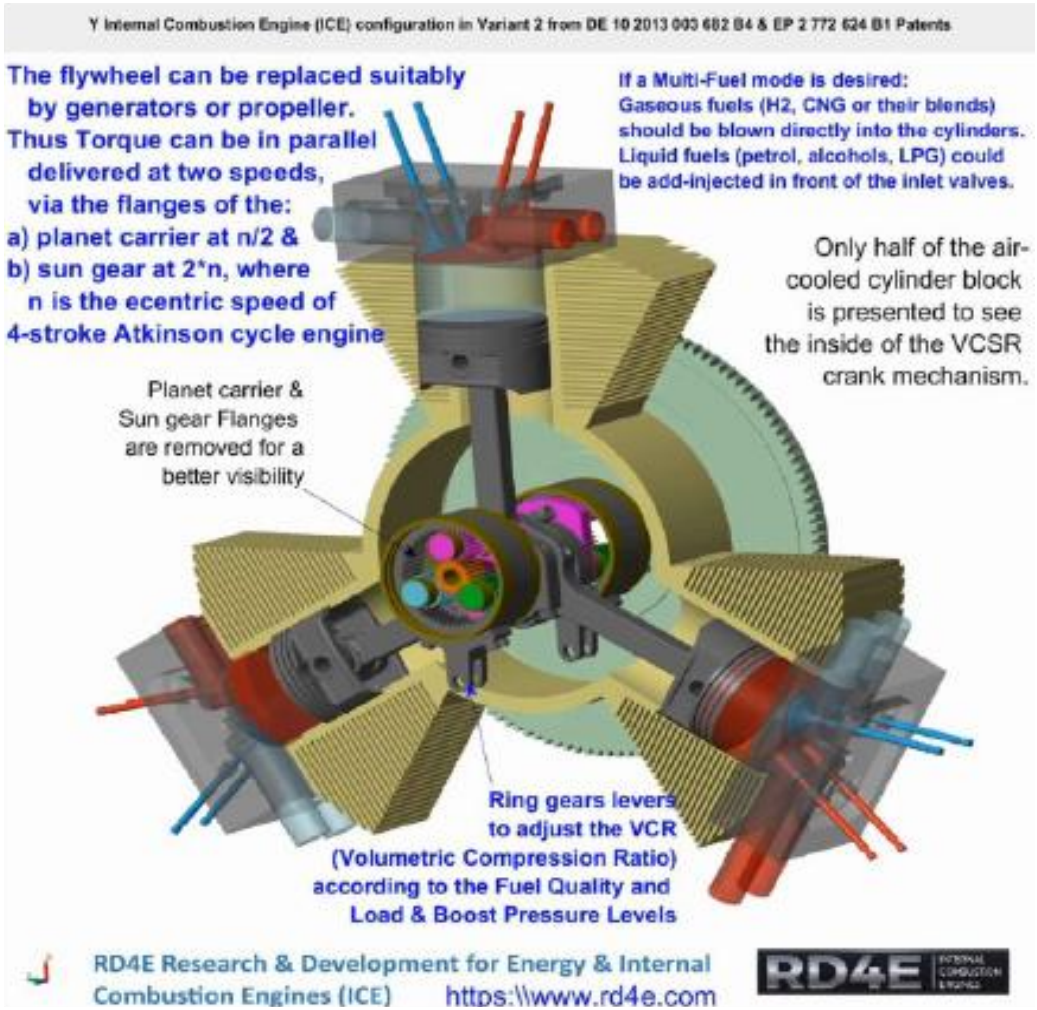


Some inward details of the 3L crank mechanism, such as the internal Gearing of CD 1, the Planet Carrier (PC 2) and inner Gearing of CD 2.
Further details can be seen in the videos above left and right, using ctrl+click !

PDV Variant 2, 3L & 3Y



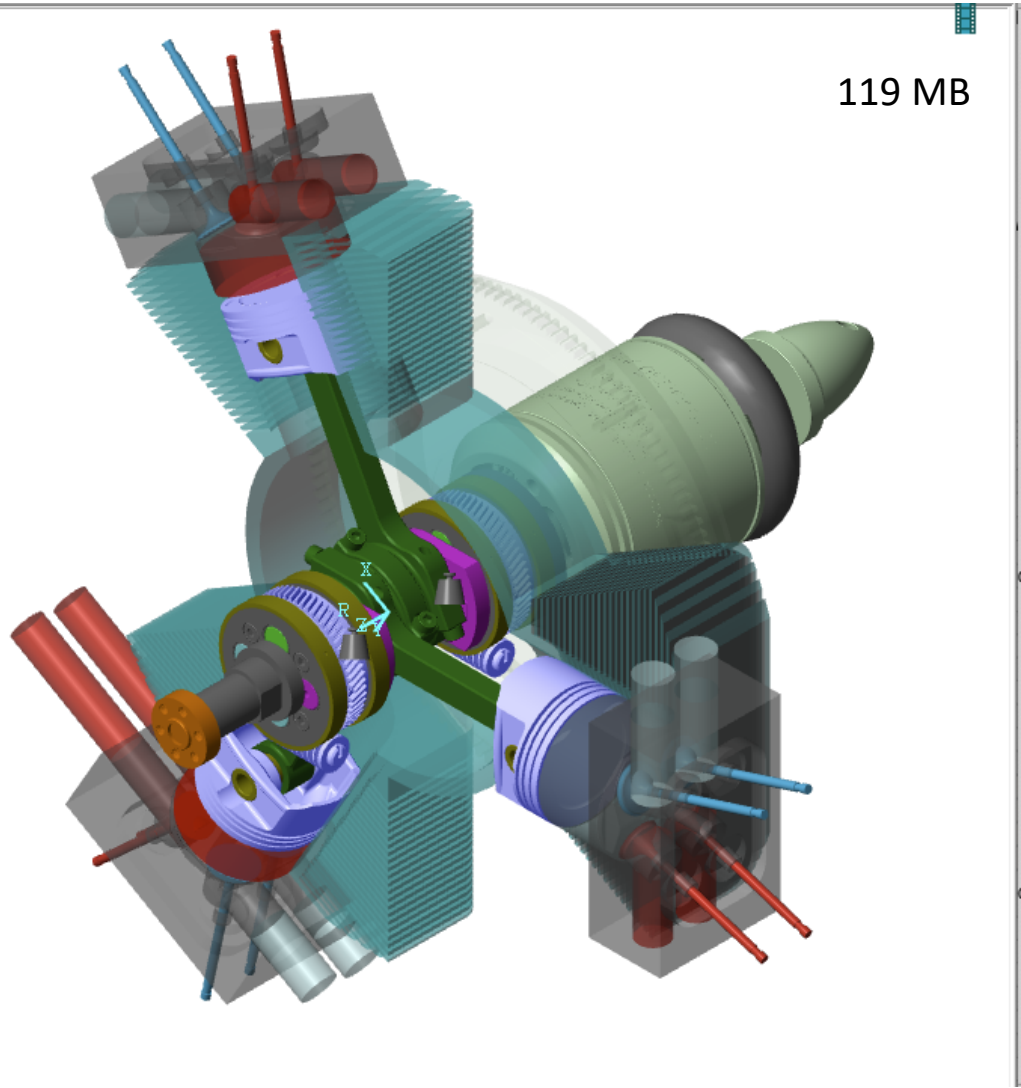
Some inward details of the **3L** crank mechanism, such as the Eccentric Crank EC 1 of the 1st cylinder and the right side of EC 2.

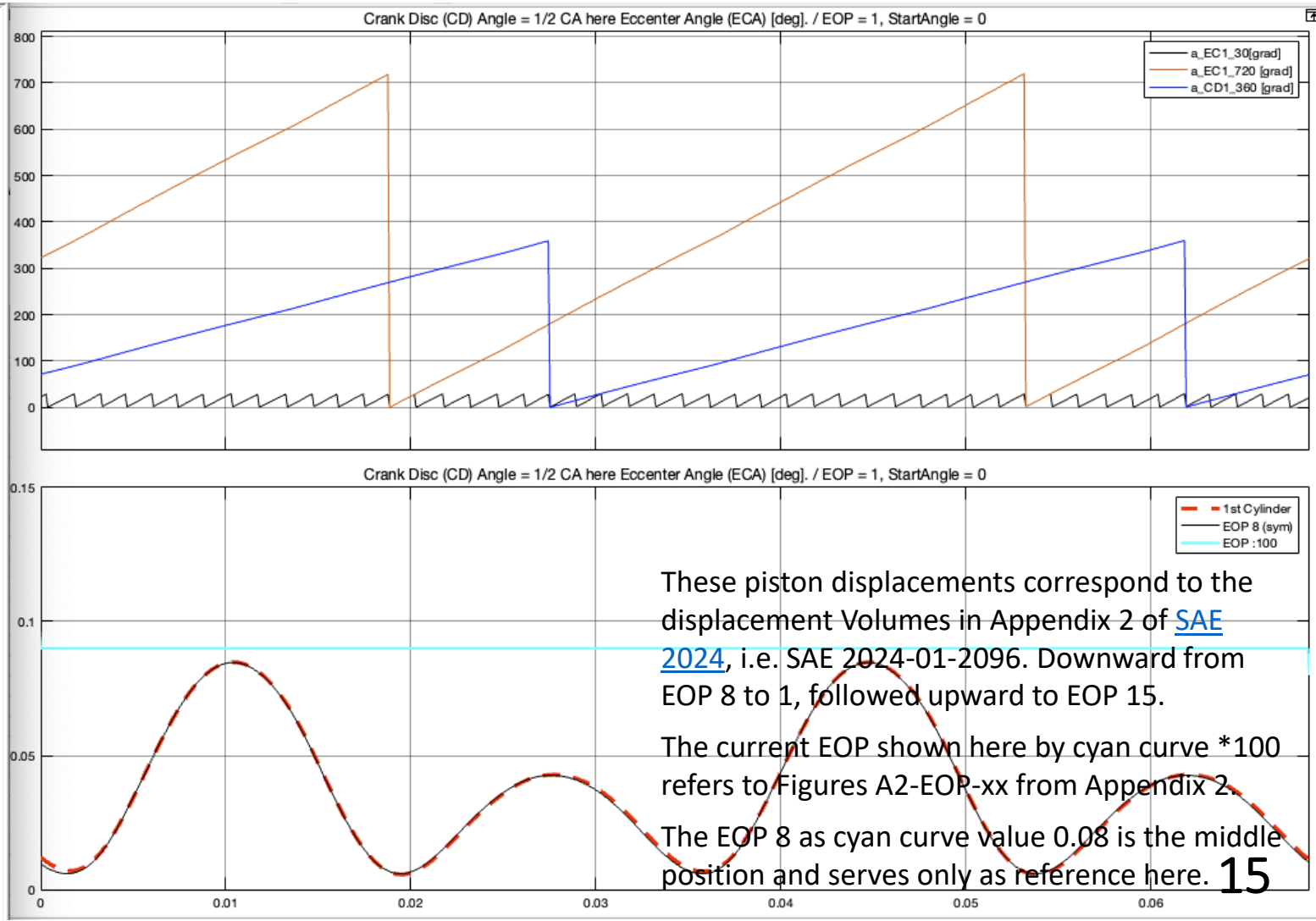


Some inward details of the Gearing of the **3Y** crank mechanism. Many 3Y cylinder groups can be in lined, as shown in the 3L configuration.

How is the VCR adjusted in PDV Variant 2 of VCRS ICE :

In this video, the VCR is varied across all 15 EOPs. The rotational position of the worm gear can be seen from the notches in the shaft and ring gear. The rotating weights for mass balancing are connected to the planetary shaft opposite the eccentric. The top scope window shows the eccentric crank angle (red), the CD angle (blue), and 30-degree intervals (black) for discretizing the time axis in seconds. The speed of the eccentric is 3500 rpm and that of the CD is half that. The bottom shows the piston displacements at different EOPs in (red) and as a reference at EOP 8 (black). The cyan curve represents current EOP divided by 100 for a right scaling.





These piston displacements correspond to the displacement Volumes in Appendix 2 of SAE 2024, i.e. SAE 2024-01-2096. Downward from EOP 8 to 1, followed upward to EOP 15.

The current EOP shown here by cyan curve *100 refers to Figures A2-EOP-xx from Appendix 2.

The EOP 8 as cyan curve value 0.08 is the middle position and serves only as reference here.

Multi-fuel based long-range Mobility for Heavy-duty drive systems e.g. in Tracked Vehicles

The drive systems of the Leopard 2 and the Abrams M1A1 serve here as references.

Liste von Dieselmotoren für schwere militärische Rad- und Kettenfahrzeuge

Motortyp	Nennleistung kW (PS)	Drehzahl min^{-1}	Maße L × B × H mm	Masse kg (trocken)	Bohrung/Hub mm	Hubraum je Zyl.	Zylinder/ Hubraum	Bemerkung
MB 838 Ka-501	1030 (1400)	2400	1738 × 1850 × 965	19				
MB 871 Ka-501	814 (1100)	*n. v.*	*n. v.*	*n*				
MB 871 Ka-501	880 (1200)	2600	1350 × 1955 × 1085	17				
MB 871 Ka-502	882 (1200)	2600	1349 × 1955 × 1085	17				
MB 873 Ka-501	1100 (1500)	2600	1801 × 1975 × 1030	22				
MB 873 Ka-501	1325 (1800)	2600	1800 × 1975 × 1060	22				



MTU-PowerPack vom Typ MB 873 Ka-501 mit Ladeluftkühlung und zwei Turboladern auf der Basis eines V12-Viertakt-Dieselmotors mit einer Leistung von 1100 kW (1500 PS)

The **Avco-Lycoming AGT1500** is a gas turbine engine. It is the main powerplant of the M1 Abrams series of tanks. The engine was originally designed and produced by the Lycoming Turbine Engine Division in the Stratford Army Engine Plant. In 1995, production was moved to the Anniston Army Depot in Anniston, Alabama, after the Stratford Army Engine Plant was shut down.[1]

Specifications [edit]

Engine output peaks at 1,500 hp (1,100 kW), with 2,750 lb·ft (3,730 N·m) of torque at that peak,[2] which occurs at 3,000 rpm.[3] The turbine can provide torque in excess of 667 lb·ft (904 N·m) at significantly lower RPMs. The engine weighs approximately 2,500 lb (1,100 kg) and occupies a volume of 40 cu ft (1.1 m^3), measuring 63 in × 40 in × 28 in (1,600 mm × 1,020 mm × 710 mm).[4]

AGT1500



U.S. Marines load an AGT1500 engine back into an M1A1 Abrams tank at Camp Coyote, Kuwait in February 2003.

Type	Turboshaft gas turbine
National origin	United States
Manufacturer	Lycoming Engines Honeywell Aerospace
Major applications	M1 Abrams

The engine can use a variety of fuels, including jet fuel, gasoline, diesel and marine diesel.[2]

The engine is a three-shaft machine composed of five sub-modules:[4]

1. Recuperator – a fixed cylindrical regenerative heat exchanger that extracts waste heat from the exhaust gases and uses it to preheat the compressed air
2. Rotating Gas Producer – the five-stage, dual-spool compressor which achieves a 14.5:1 compression ratio at full power, driven by the compressor turbine, which operates with a maximum turbine inlet temperature of 2,180 °F (1,190 °C)
3. Accessory Gearbox – bevel gears that extract 35 to 100 hp (26 to 75 kW) from the high-pressure spool to operate the fuel control unit, starter, oil pump, and vehicle hydraulic pump
4. Power Turbines – the first stage of the two-stage power turbine is driven by a variable-geometry nozzle to improve efficiency
5. Reduction Gearbox – reduces power turboshaft speed

Multi-fuel based long-range Mobility for Heavy-duty drive systems e.g. in tracked & wheeled Vehicles

Some examples:













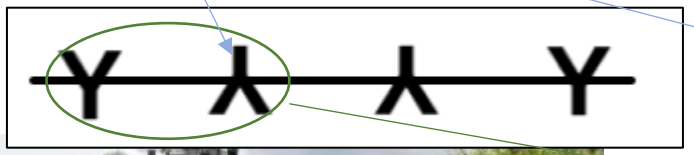


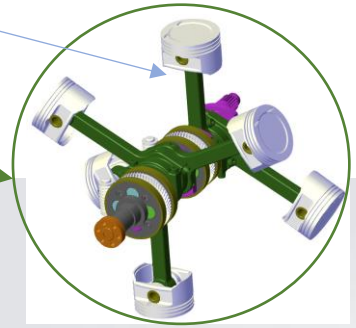


Multi-fuel based long-range Mobility for Heavy-duty drive systems e.g. in tracked & wheeled Vehicles



Heavy-duty drive systems, as shown before and below, cannot be driven by a simple 3Y VCSR unit. A series of many 3Y units is required. This series consisting of 3Y and 180° rotated 3Y, as shown in figure below, provide an optimal mass balance e.g. for a 12-cylinder engine:





In contrast to heavy-duty app, a simple 3Y VCSR could be sufficient for such terrestrial drones, as shown above.







Single-fuel based long-range Mobility for Light Aircraft Systems

Several valve control systems for gas exchange are known for internal combustion engines.

- 4-stroke engines typically use poppet valves.
- Ricardo invented and promoted sleeve valves controlled by cylinder rotation.
- 2-stroke engines usually have either slots for intake and exhaust or, especially in large engines, slots for intake and poppet valves for exhaust.
- Rotary engines (e.g. Wankel) use slide slits

The **Rotax 915 iS** is an Austrian aircraft engine, produced by Rotax of Gunskirchen for use in ultralight aircraft, homebuilt aircraft, light-sport aircraft, small helicopters and gyroplanes. The engine was type certified in 2017.[2][3]

The engine was first publicly displayed at AirVenture in July 2015[2] and first flown in March 2016.[4]

In January 2016 the engine was named AVweb's "Best New Engine" of 2015.[5]

Design and development [edit]

The Rotax 915 iS is a four-cylinder four-stroke, horizontally-opposed, turbocharged, air and liquid-cooled, gasoline engine design, with a mechanical gearbox reduction drive. The turbocharger has a compression ratio of 3.5:1 and the engine will have a critical altitude of 15,000 ft (4,572 m). It employs dual electronically controlled fuel injection, using dual channel Rockwell Collins ECUs, with dual ignition and produces 141 hp (105 kW) for take-off and 135 hp (101 kW) continuous. The engine can produce rated power up to 15,000 ft (4,572 m) and has a ceiling of 23,000 ft (7,010 m).[1][2][6]

The engine is based on the Rotax 912, but differs in that it has fuel injection, a reinforced crankshaft, new pistons, a new gearbox and a turbocharger. Time between overhauls was expected to eventually be raised to 2000 hours with operational experience, but started at 1200 hours.[2][6][1]

The design entered production in the second half of 2017. The European Aviation Safety Agency certified the Rotax 915 iSc3 A on 14 December 2017 and the Rotax 915 iSc3 B on 4 January 2018.[7]

In December 2021 the option to replace the 12V electrical system with a 24V one was introduced. The 24V version of the engine is designated the 915iS C24 for the non-certified version and the 915iSc C24 certified version.[8]

Rotax 915 iS

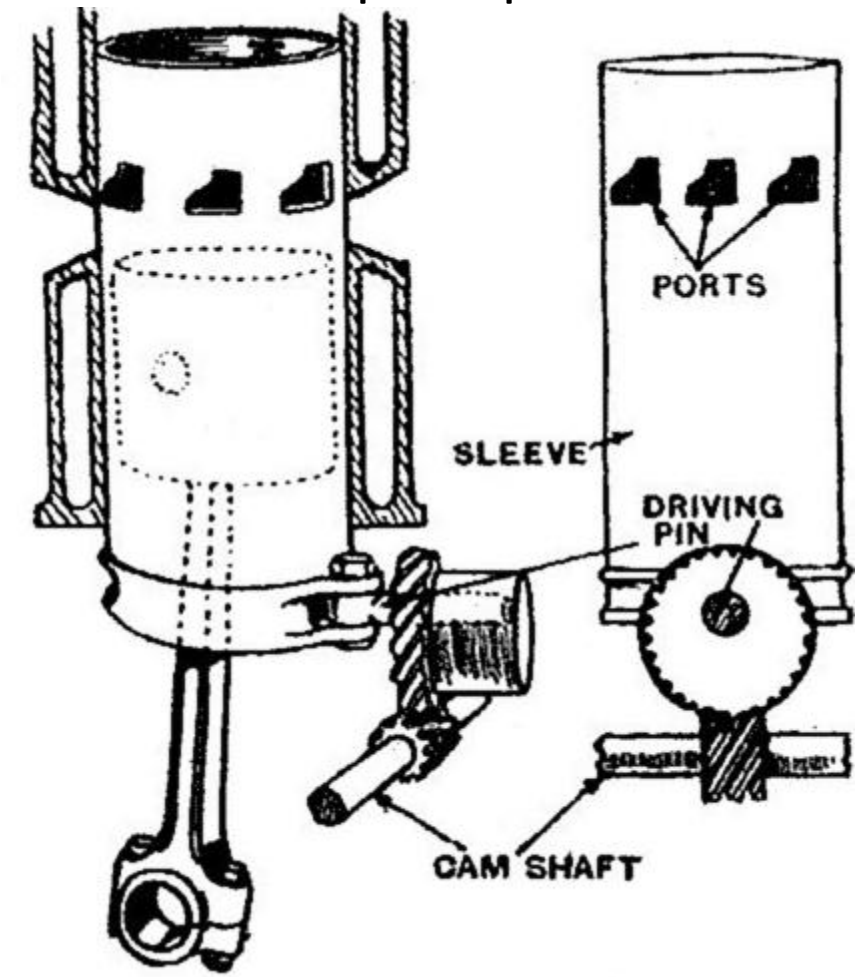


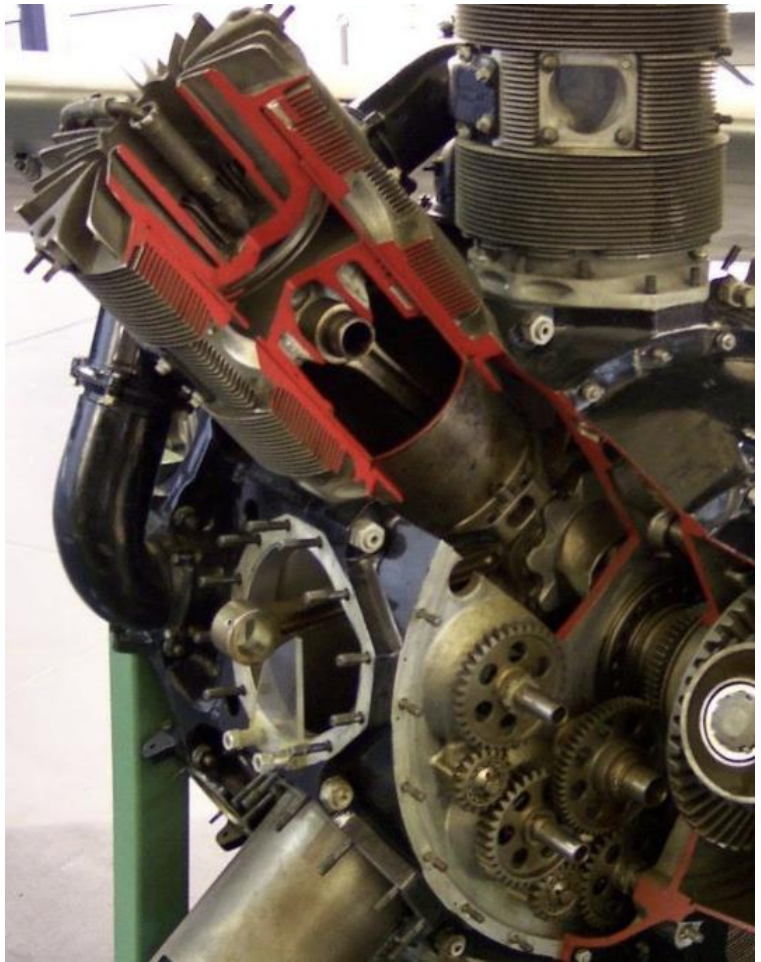
Type	Piston aircraft engine
National origin	Austria
Manufacturer	Rotax
First run	2014
Major applications	Issoire APM 41 Simba 915iS
Produced	2017-present[1]
Developed from	Rotax 912
Variants	Rotax 916 iS

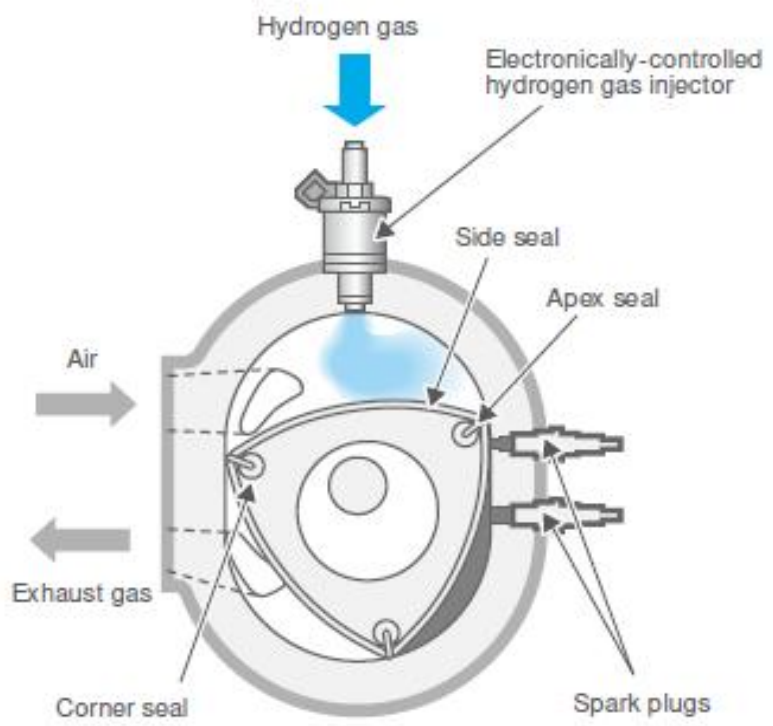
Single-fuel based long-range Mobility for Light Aircraft Systems

On the right is a cross-section of the Wankel engine, shown here as Mazda RENESIS, with side slits for air and exhaust gases.
Below is part of the Bristol Perseus engine with sleeve valves.

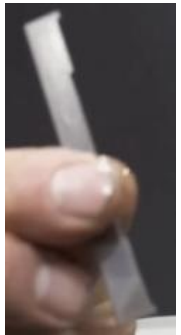
Sleeve valve principle of Sir Harry Ricardo.







Type	Mazda RENESIS hydrogen rotary engine with ISG
Maximum power	Using Gasoline: 154 kW (210 PS) @7200 rpm Using Hydrogen: 81 kW (110 PS) @7200 rpm (target)
Maximum torque	Using Gasoline: 222 N·m@5000 rpm Using Hydrogen: 120 N·m@5000 rpm (target)





Long-range Mobility for Light Aircraft Systems based on multiple fuels through the use of VCSR instead of current engines

Model VoloCity of Volocopter company



Drone Heron TP





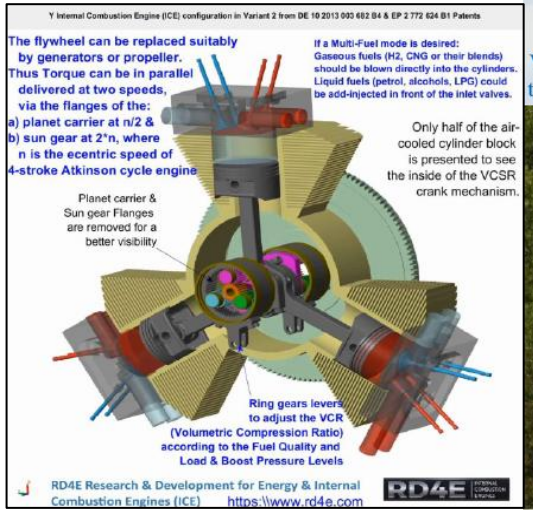
Black Hornet 4

Drone Luna



Proposed modifications for reaching of long-range operation capabilities







Range estimation for Light Aircraft Systems based on hydrogen fuel through the use of VCSR as range extender instead of current pure electric drive

Table 7-1. Published, estimated, assumed and computed parameter of some Flight-Taxis eVTOLs.

Parameter	Unit	Symbol	E-Hang 184	CityAirbus	Volocity	Lilium [22]	Source
Maximum E Motors Power	kW	P_EM	106	800	270	360	estimated
Number of E Motors (Fans)		n_EM	8	8	18	36	published
Total Batteries Energy	kWh	E_batt	14.4	110	39	95	
Battery Power = P_batt_m *m_batt	kW	P_batt	67.4	515.0	182.6	610.1	computed
Net Mass	kg	m_net	260	1800	700	1700	
Capacity, Number of Pax + Pilot		n_pax	1	4	2	5	
Rated Payload Weight (RPW)	kg	m_pax	100	400	200	500	
Maximal Take-off Mass (MTOM)	kg	m_max	360	2200	900	2200	
Autonomy, Total Flight Time	min	t_flight	23	15	15	55	
Flight Range	km	L_range	35	35	35	245	
Averaged Flight Speed, Cruise Speed	km/h	v_cruise	100	120	110	290	
Battery Mass = E_batt / E_batt_m	kg	m_batt	92	701	248	830	assumed
Battery energy specific density	kWh/kg	E_batt_m	0.157	0.157	0.157	0.157	by Tesla
Battery power density	kW/kg	P_batt_m	0.735	0.735	0.735	0.735	by Tesla
E_batt/m_max	kWh/kg		0.040	0.050	0.043	0.043	estimated
P_EM/m_max	kW/kg		0.29	0.36	0.30	0.16	
single E Motor Power	kW	P_1EM	13.25	100	15	10	
m_batt/m_net	%		35.3	38.9	35.5	48.8	

Potential Hydrogen Fueling Capacity of the Volocopter (an estimation)

$W_{hooves} := 2 \cdot m$ Distances between hooves

$L_{hooves} := 2.1 \cdot m$ Hooves lenght

$H_{hooves} := 0.7 \cdot m$ Hooves high

$V_{H2} := W_{hooves} \cdot L_{hooves} \cdot H_{hooves}$ Maximal Hydrogen Tanks volums between the hooves

$V_{H2} = 2.94\,m^3$

$\eta_{iVCSR} := 0.5$ indicated Efficiency of the VCSR ICE

$\eta_m := 0.95$ mechanical Efficiency of the VCSR ICE and electric motors and other losses

$\eta_e := \eta_{iVCSR} \cdot \eta_m$ $\eta_e = 0.475$ effective Efficiency

$H_{uH2} := 120 \cdot \frac{MJ}{kg}$ H_2 lower heating value, see Table 1

$\rho_{H2_350bar} := 24 \cdot \frac{kg}{m^3}$ Hydrogen Density at 350 bar, see Fig. 12

$\rho_{H2_700bar} := 40 \cdot \frac{kg}{m^3}$ Hydrogen Density at 700 bar, see Fig. 12

$m_{H2_350bar} := V_{H2} \cdot \rho_{H2_350bar}$ $m_{H2_350bar} = 70.56\,kg$ available H_2 Mass

$m_{H2_700bar} := V_{H2} \cdot \rho_{H2_700bar}$ $m_{H2_700bar} = 117.6\,kg$

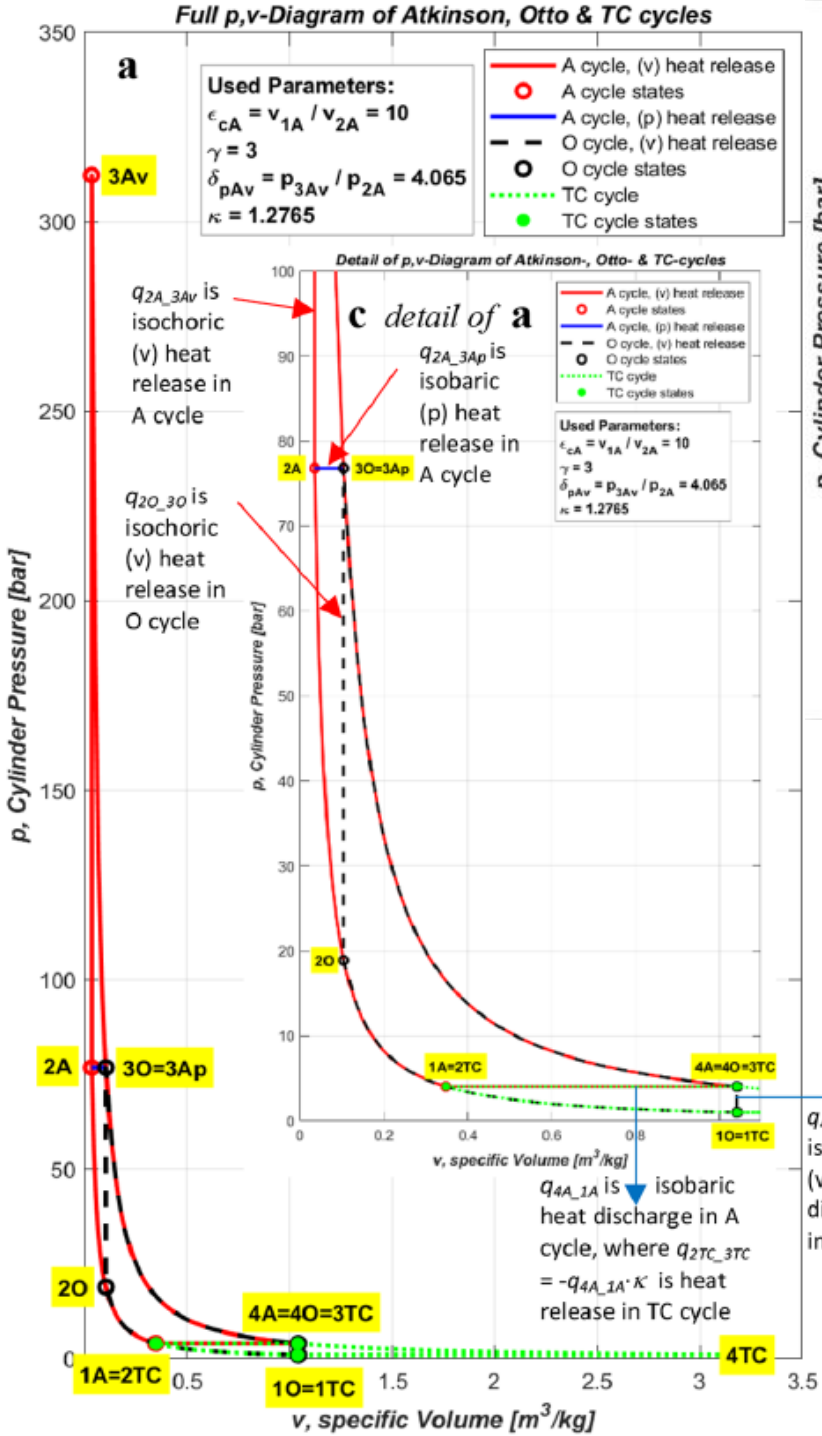
$E_{H2_350bar} := m_{H2_350bar} \cdot H_{uH2} \cdot \eta_e$ $E_{H2_350bar} = 1.117 \times 10^3\,kWh$ available H_2 Energy

$E_{H2_700bar} := m_{H2_700bar} \cdot H_{uH2} \cdot \eta_e$ $E_{H2_700bar} = 1.862 \times 10^3\,kWh$

CityAirbus reachs with 110 kWh battery capacity a range of 35 km.
The situation by Volocity is nearly the same! That means the ranges by using VCSR ICE and Hydrogen in place of battery could be:

$Range_{350bar} := \frac{E_{H2_350bar}}{110 \cdot kWh} \cdot 35 \cdot km$ $Range_{350bar} = 355.473\,km$

$Range_{700bar} := \frac{E_{H2_700bar}}{110 \cdot kWh} \cdot 35 \cdot km$ $Range_{700bar} = 592.455\,km$



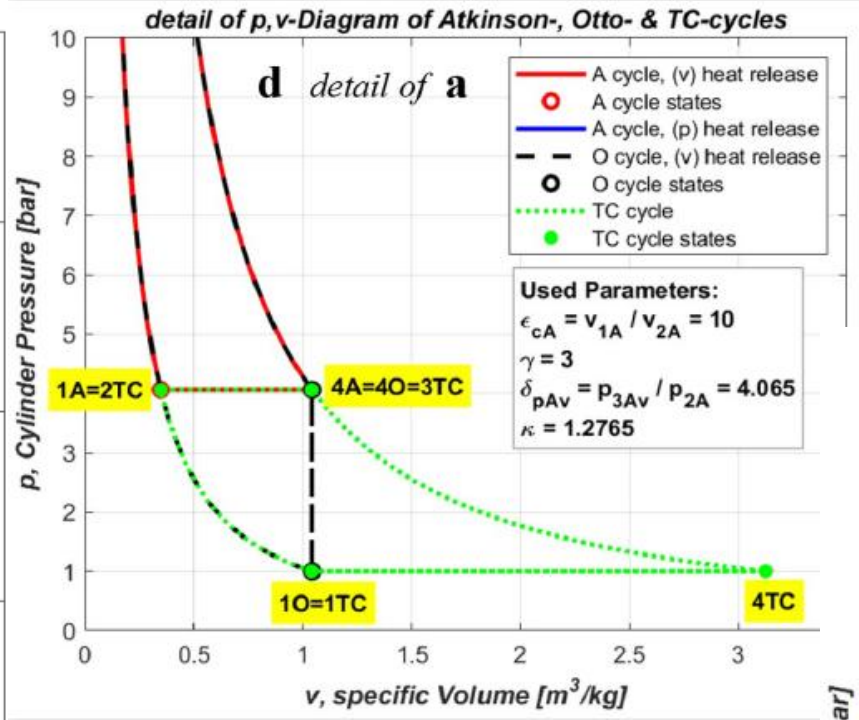


Fig. A2-1 / page 28 of SAE 2024-01-2096

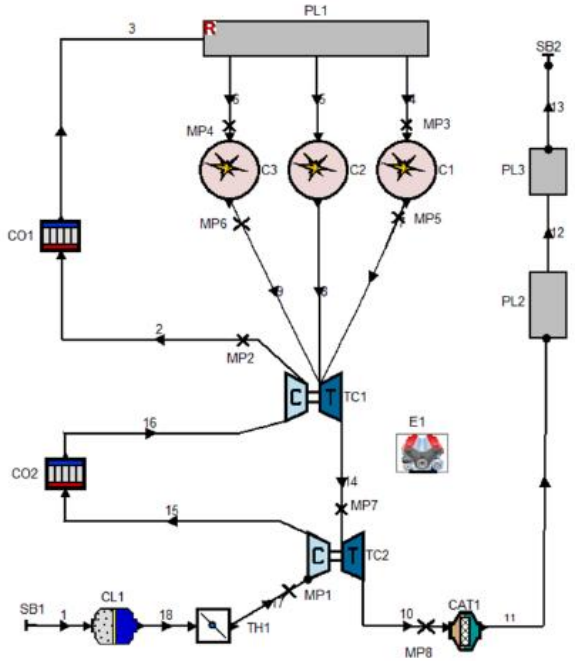
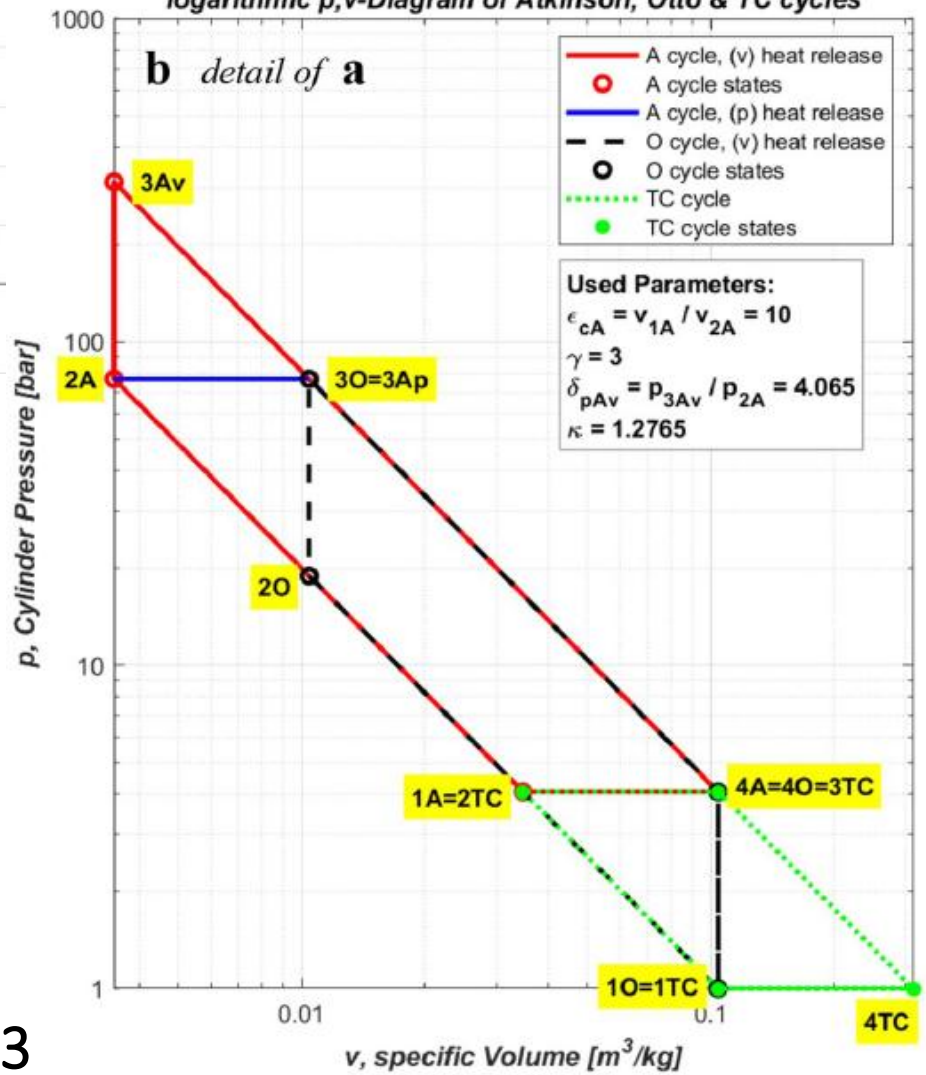


Fig. 5, 6, 7 / pages 7, 8 of SAE 2024-01-2096

Thermodynamics
continuation



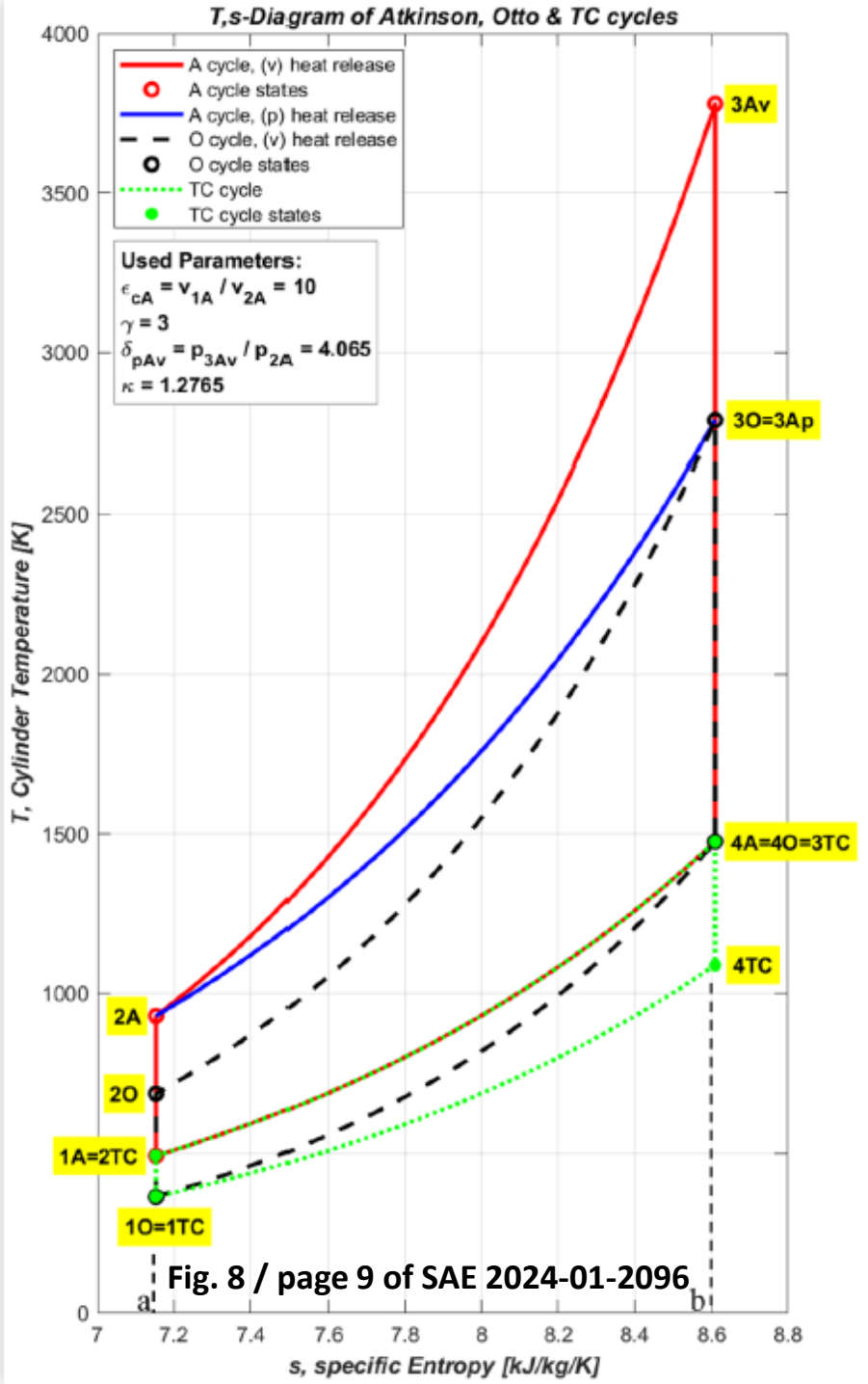


Fig. 8 / page 9 of SAE 2024-01-2096

The IFCE of the true Atkinson A cycle with isochoric heat release depends on VCR and κ but also on δ_p and γ.

$$\eta_{thA_v} = 1 - \frac{1}{(\epsilon_c \cdot \gamma)^{\kappa-1}} \cdot \frac{\delta_p - \gamma^{\kappa-1}}{\delta_p - 1}$$

Further formula is obtained after eliminating of δ_p using the relation $\delta_p = \gamma^\kappa$. The proof of this relation is provided by the p,v-diagrams from Figs. 2 and 6 and following thermodynamic correlations:

The state changes 1A-2A and 3A-4A occur isentropically, thus

$$\epsilon_c = \frac{V_{2A}}{V_{1A}} \qquad \epsilon_e = \frac{V_{4A}}{V_{2A}} \qquad \gamma = \frac{\epsilon_e}{\epsilon_c} = \frac{V_{4A}}{V_{1A}}$$

$$p_{2A} = p_{1A} \cdot \epsilon_c^\kappa, \qquad p_{3A} = p_{2A} \cdot \delta_p, \qquad \text{i.e. } p_{3A} = p_{1A} \cdot \epsilon_c^\kappa \cdot \delta_p,$$

$$p_{3A} = p_{4A} \cdot (\epsilon_c \cdot \gamma)^\kappa, \qquad p_{4A} = p_{1A}, \qquad \text{i.e. } p_{3A} = p_{1A} \cdot \epsilon_c^\kappa \cdot \gamma^\kappa$$

Equating both expressions for p_{3A} yields the relationship we are looking for $\delta_p = \gamma^\kappa$. The IFCE of A cycle thus becomes:

$$\eta_{thA_v} = 1 - \frac{1}{(\epsilon_c \cdot \gamma)^{\kappa-1}} \cdot \left[1 + \frac{1}{\gamma^\kappa - 1} \cdot \left(1 - \gamma^{\kappa-1} \right) \right]$$

If the heat is released purely isobarically (p) after the pressure p2A = p3O has been reached, i.e. in such a way that no further increase in pressure occurs. The IFCE in this case becomes:

$$\eta_{thA_p} = 1 - \frac{1}{\kappa \cdot \epsilon_c^{\kappa-1}}$$

Summary of the Comparison of Ideal Cycles

Depending on the estimated heat release type in the Atkinson cycle, the improvement of IFCE between the Atkinson and Otto cycles, are as follows:

Isochoric heat release in A cycle **Isobaric** heat release in A cycle

$$\frac{\eta_{thA_v} - \eta_{thO_v}}{\eta_{thO_v}} = 39\% \qquad \frac{\eta_{thA_p} - \eta_{thO_v}}{\eta_{thO_v}} = 24.3\%$$

The IFCE comparison between the Atkinson cycle and the Gas Turbine (TC) cycle is very much stronger, but distorted because of the different VCR values:

$$\frac{\eta_{thA_v} - \eta_{thTC_p}}{\eta_{thTC_p}} = 149.9\% \qquad \frac{\eta_{thA_p} - \eta_{thTC_p}}{\eta_{thTC_p}} = 123.5\%$$

Even the IFCE comparison between the Otto cycle and the Gas Turbine (TC) cycle is very unfavorable for the TC cycle:

$$\frac{\eta_{thO_v} - \eta_{thTC_p}}{\eta_{thTC_p}} = 79.8\%$$

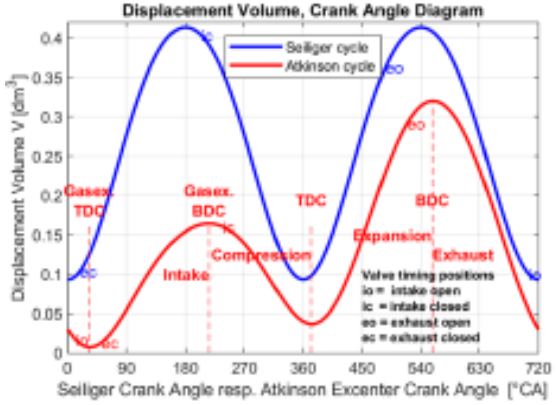
All these IFCE (efficiency) comparisons show that the Gas Turbine cycle of aircraft engines, such as turboprop and turbofan, have to be rigorously reconsidered. Their lower VCR is imposed from T_{4TC} = 1200°C and stoichiometric AFR, λ = 1, at ambient intake pressure.

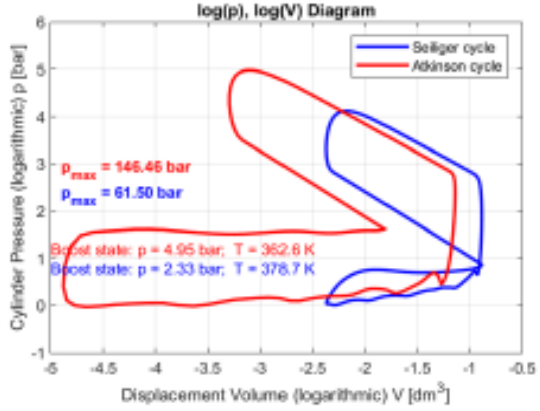
Using a VCSR engine, as the CORE instead of the burn chamber of the turbofan or turboprop aero engines will enables the following:

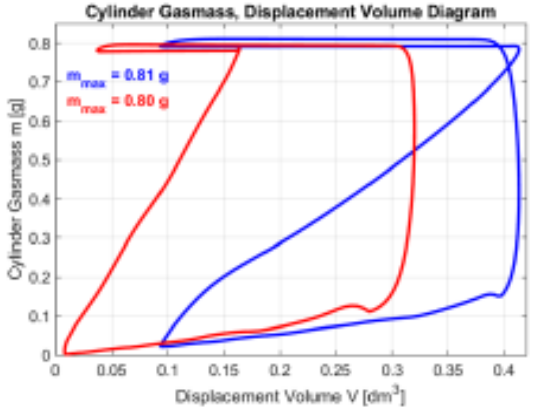
a. A huge increase in efficiency, thus drastically reducing the specific fuel consumption,
b. A much greater bypass flow, e.g. well over 20%,
c. A simpler compensation of the altitude flight by the variable VCR,
d. The use of various fuels, such as gaseous or liquefied H_2 or NH_3, biofuels, CNG, LPG or even Kerosene, either pure or in any mixture.

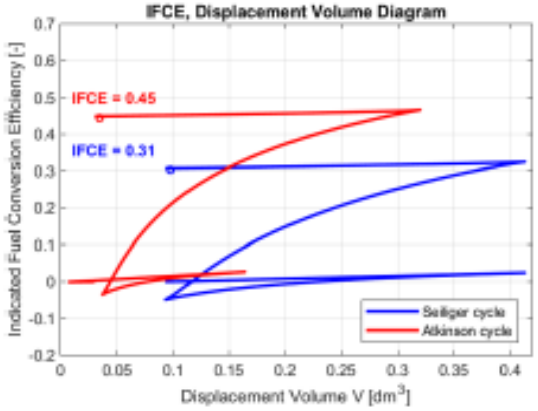
FIGURE A2-EOPS-01-15 Ultra Downsizing (UD) Load Control (LC) example

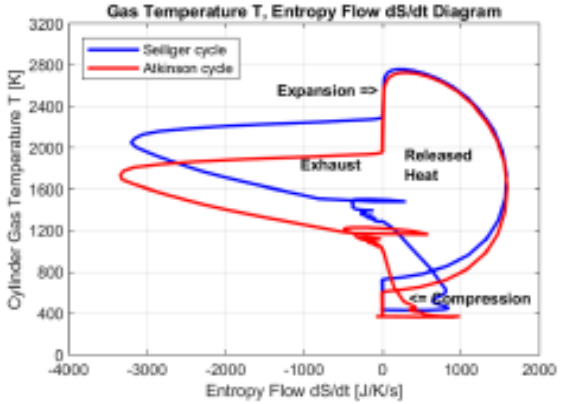
15th EOP, adiabatic & FMEP = 2.12 bar, H_2-fueled ICE, working according to Seliger and Atkinson cycles, with identical: VCR ϵ_c = 4.43, expansion stroke lengths & maximum gas mass, AFR λ = 1; γ of Atkinson cycle = 1.95 or 7° RG setting

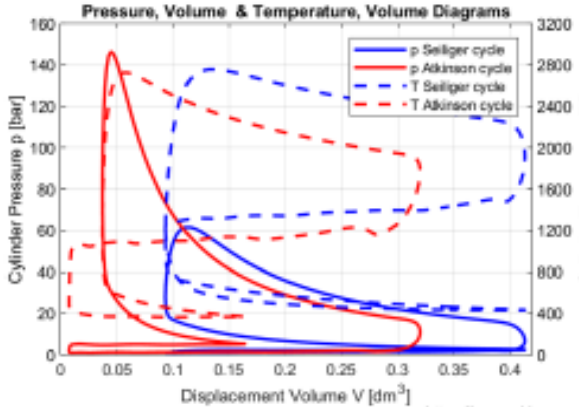




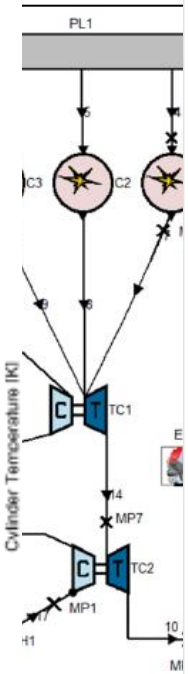




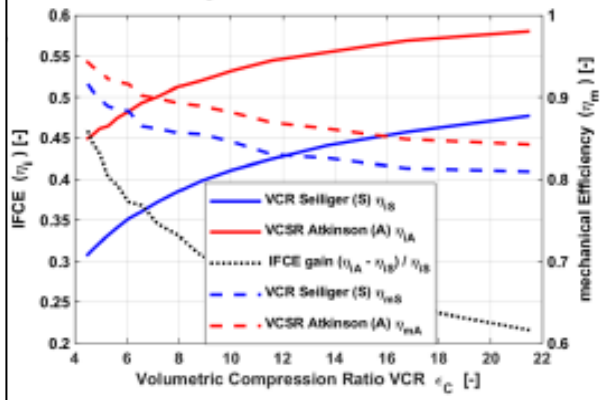


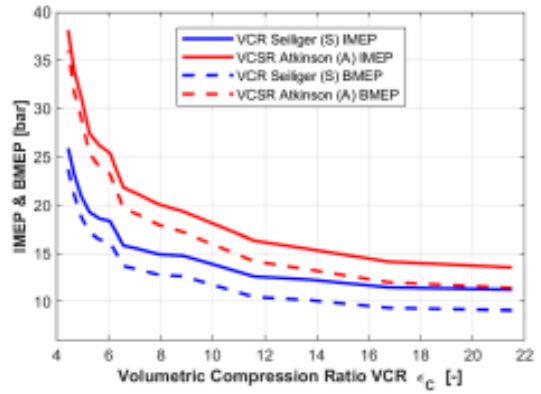


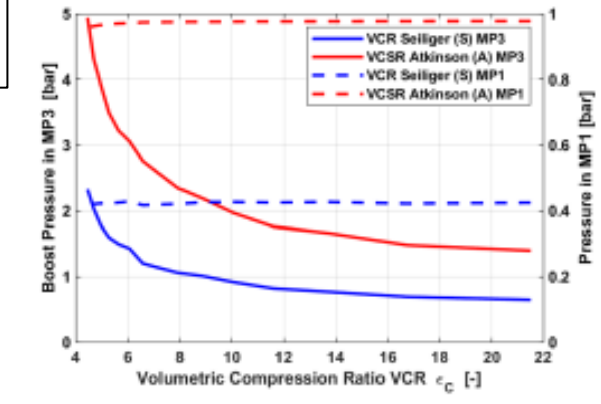
S. Next Slide for Simulation model in AVL BOOST, EOP means engine Operation Point & MP means Measuring Point

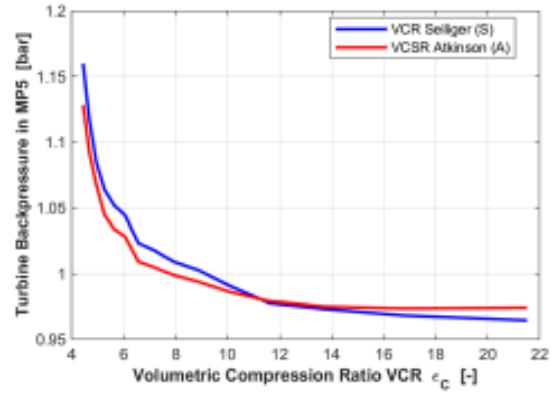


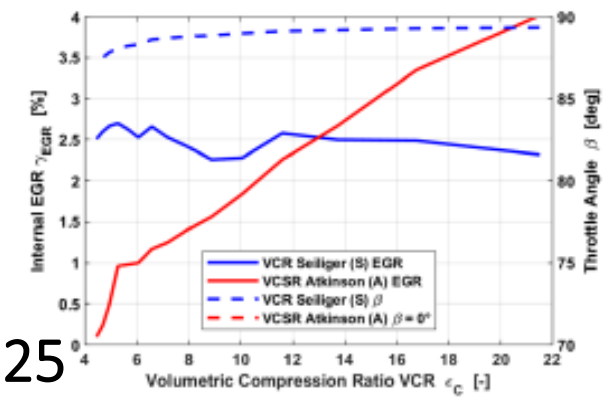
Load Excursion of adiabatic & FMEP = 2.12 bar, H_2-fueled ICEs, working according to Seliger and Atkinson cycles, with identical: VCR ϵ_c, expansion stroke lengths & maximum gas mass, AFR λ = 1; Atkinson cycle with $\gamma \cong 2$

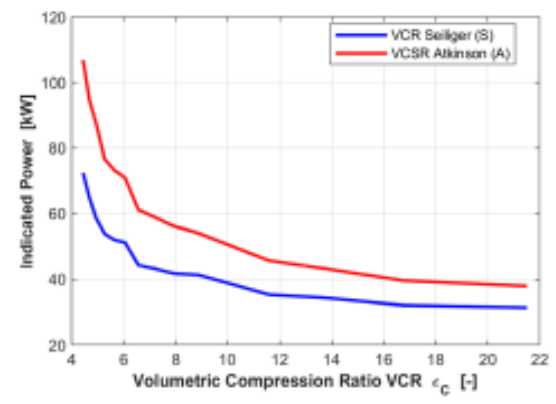




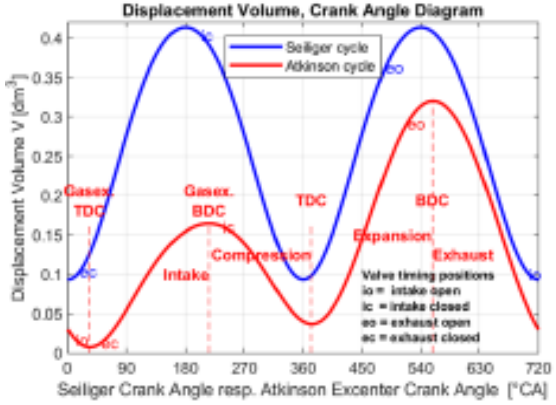








15th EOP, adiabatic & FMEP = 2.12 bar, H_2-fueled ICE, working according to Seliger and Atkinson cycles, with identical:
VCR ϵ_c = 4.43, expansion stroke lengths & maximum gas mass, AFR λ = 1; γ of Atkinson cycle = 1.95 or 7° RG setting



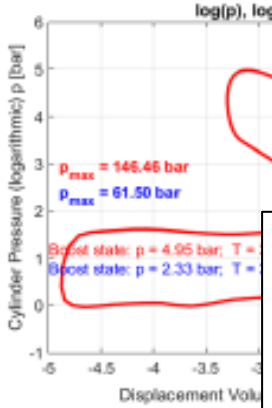


Fig. A2-1 / page 28 of SAE 2024-01-2096
Simulation model in AVL BOOST
EOP means engine Operation Point &
MP means Measuring Point

FIGURE A2-EOPS-01-15 Ultra Downsizing (UD) Load Control (LC) example

Load Excursion of adiabatic & FMEP = 2.12 bar, H_2-fueled ICEs, working according to Seliger and Atkinson cycles, with identical:
VCR ϵ_c, expansion stroke lengths & maximum gas mass, AFR λ = 1; Atkinson cycle with $\gamma \cong 2$

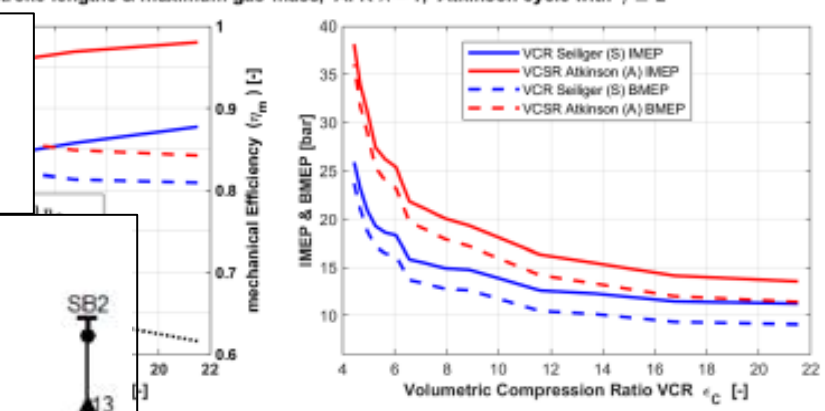
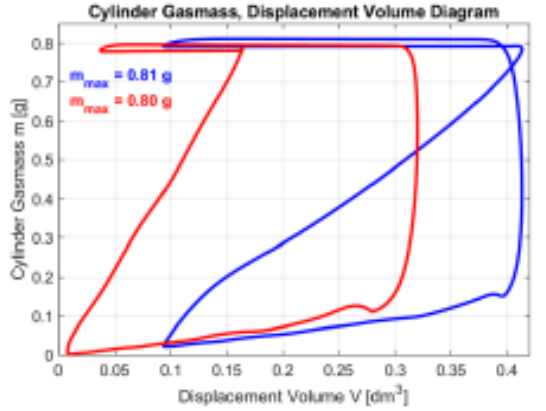
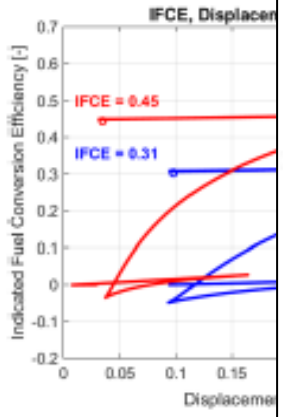
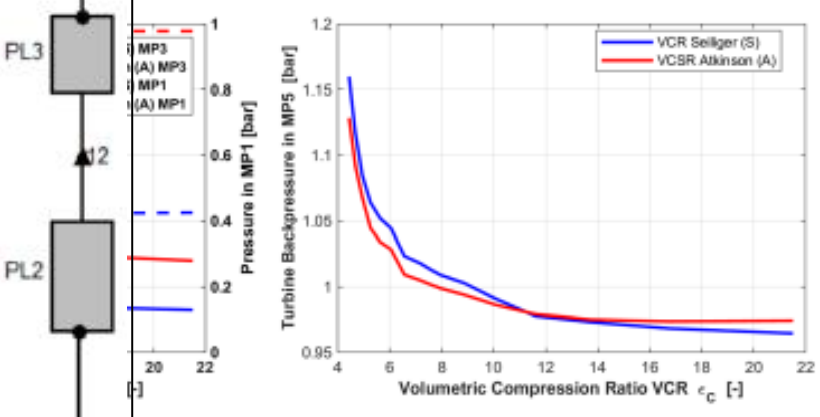


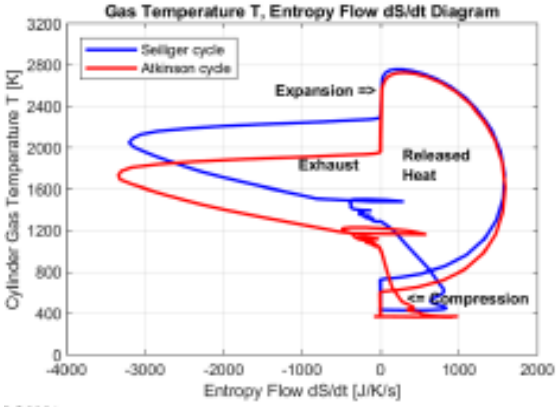
Fig. A2-EOP-15 / page 45 of SAE

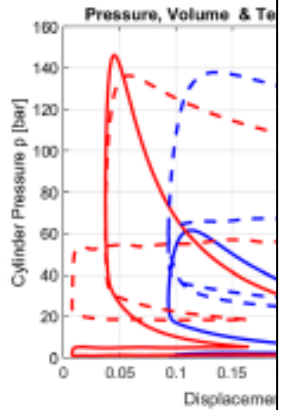
46 of SAE 2024-01-2096

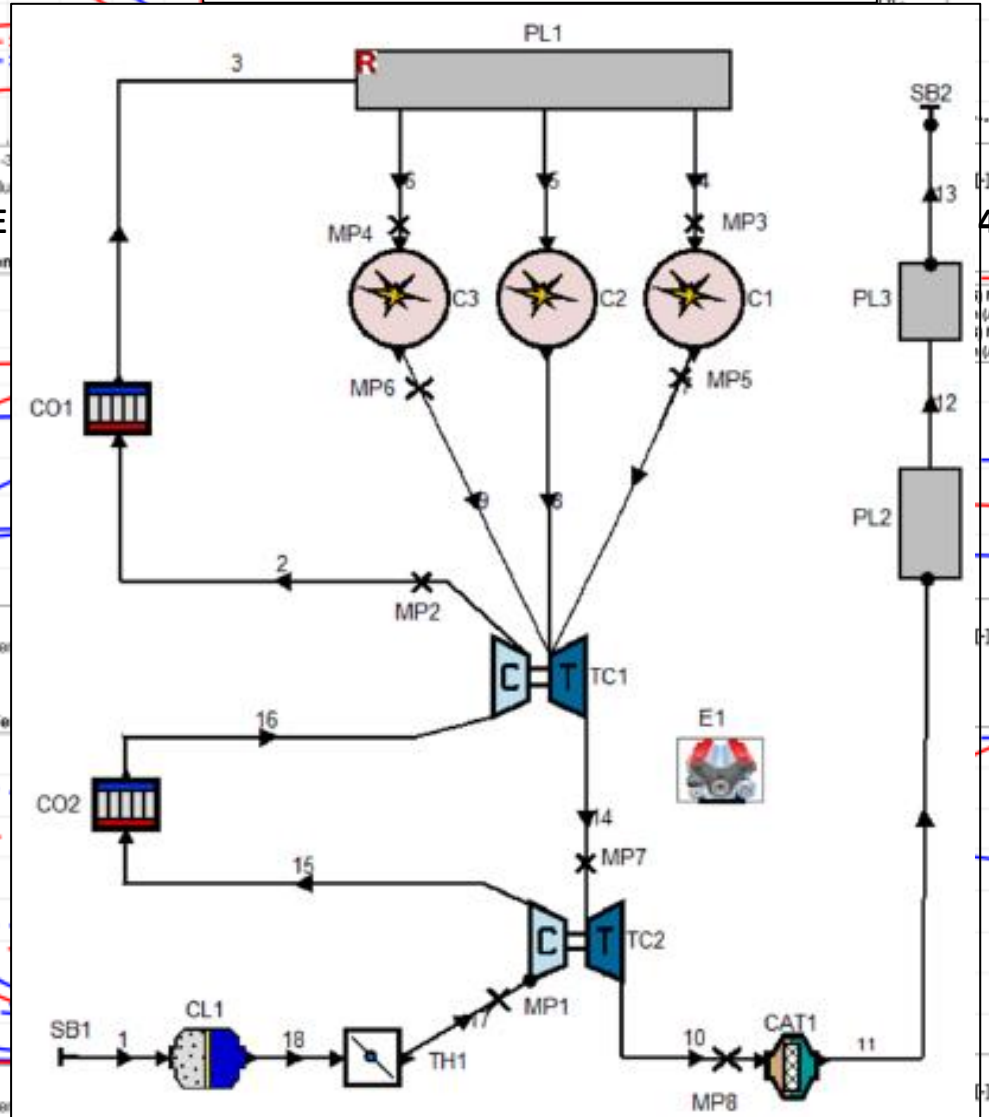


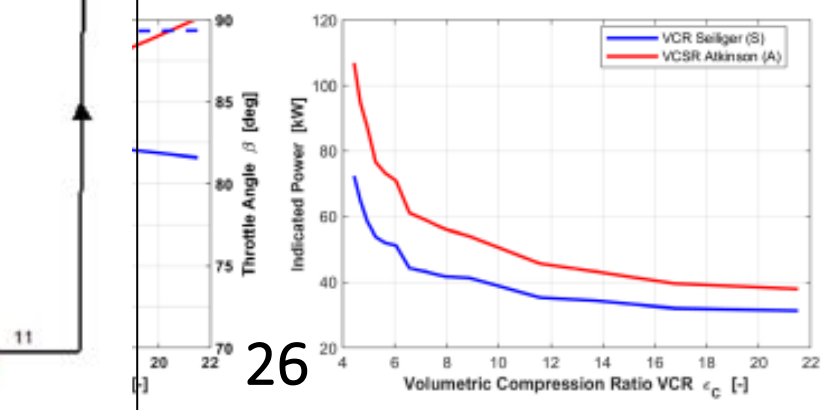












Multi-fuel based sustainable long-range Mobility

➢ Analysis of Fuels and their possible uses

Some facts about the multi-fuel capabilities are shown in the section: Multi-Fuel_Seiten aus SAE_21ICE-0132.pdf

The table of properties of the known fuels shows that

- ➢ none of them is perfect and
- ➢ offers only application advantages for specific use.
- ➢ Ammonia is much more suitable as Hydrogen because of its higher LHV per volume, if CO_2 free emissions are desired.

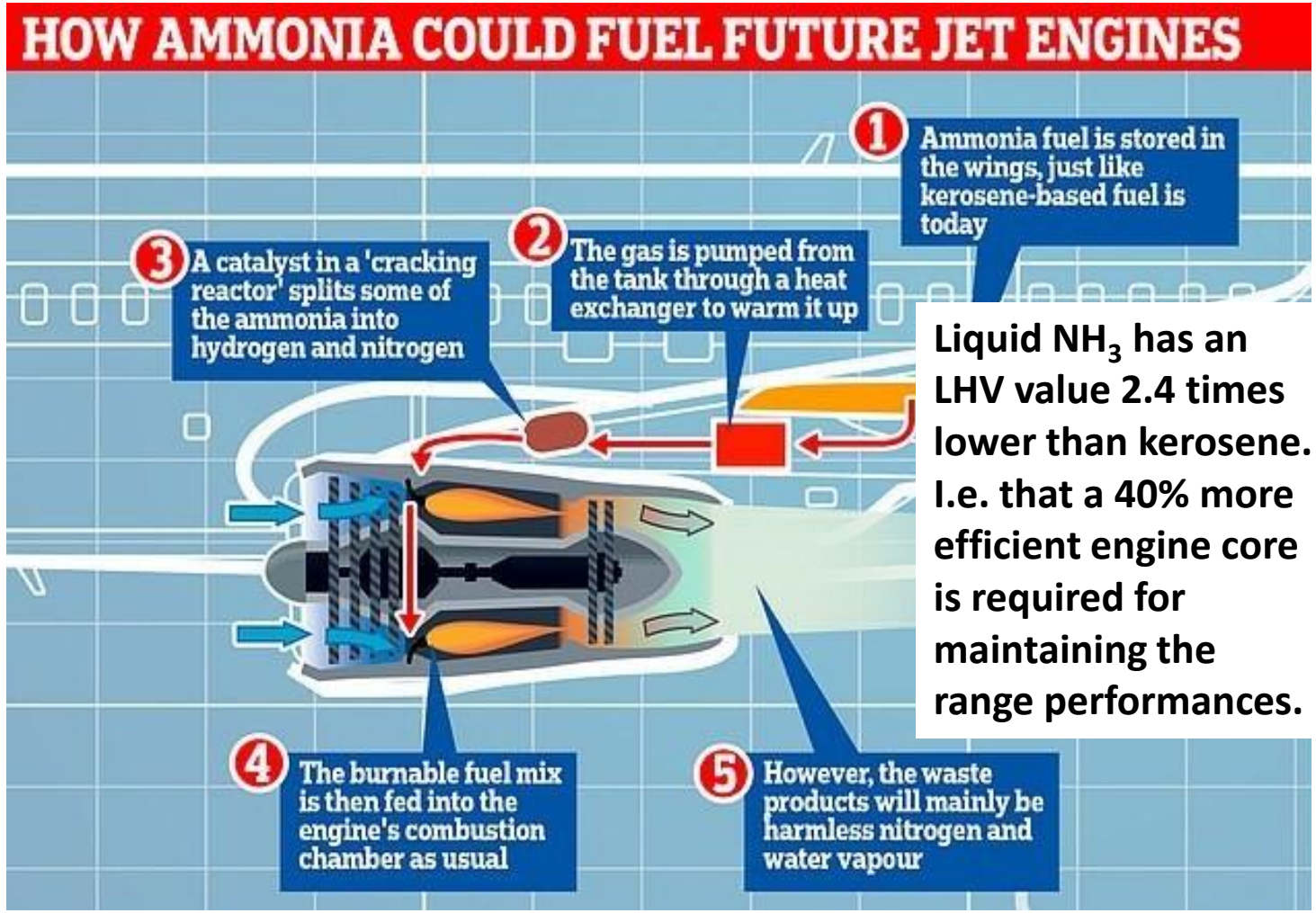
Traditional fuels such as Gasoline and Diesel, which have a relatively high Lower Heat Values LHV per mass and volume, produce too much CO_2 after combustion. Although this is not crucial for military purposes, it should nevertheless be taken into account.

	Energy content (LHV) [MJ/Kg]	Energy content (LHV) [MJ/L]	Density [kg/m^3]	Octane [RON]	Flame-velocity [m/s]	Flammability-limits [vol/%]	Minimum Ignition Energy [mJ]
Cooled Ammonia (Liquefied)	18.6	12.69 (1 atm, -33°C)	682	>130	0.067	15-28	680
Compressed Ammonia (Liquefied)	18.6	11.65 (300 bar ,25°C)	626.	>130	0.067	15-28	680
Cooled Hydrogen (Liquefied)	120	8.5 (1atm, -253°C)	70.85	>130	3.25	4.7-75	~0.016
Compressed Hydrogen (gaseous)	120	2.46 (300 bar, 25°C)	20.54	>130	3.25	4.7-75	~0.016
Diesel (n-dodecane)	44.11	32.89 (1 atm, 25°C)	745.7[12]	<20	~0.80	0.43-0.6	~0.23
Gasoline (iso-octane)	44.34	(n-octane) 30.93 (1 atm,25°C)	(n-octane) 697.6	100	0.41 ~0.58 (RON 90-98)	0.95-6 0.6-8 (RON 90-98)	1.35 ~0.14 (RON 90-98)
Methanol	19.90	15.65 (1 atm,25°C)	786.3	108.7	0.56	6.7-36	~0.14
Ethanol	26.84	21.07 (1 atm,25°C)	785.1	108.6	0.58	3.3-19	0.6

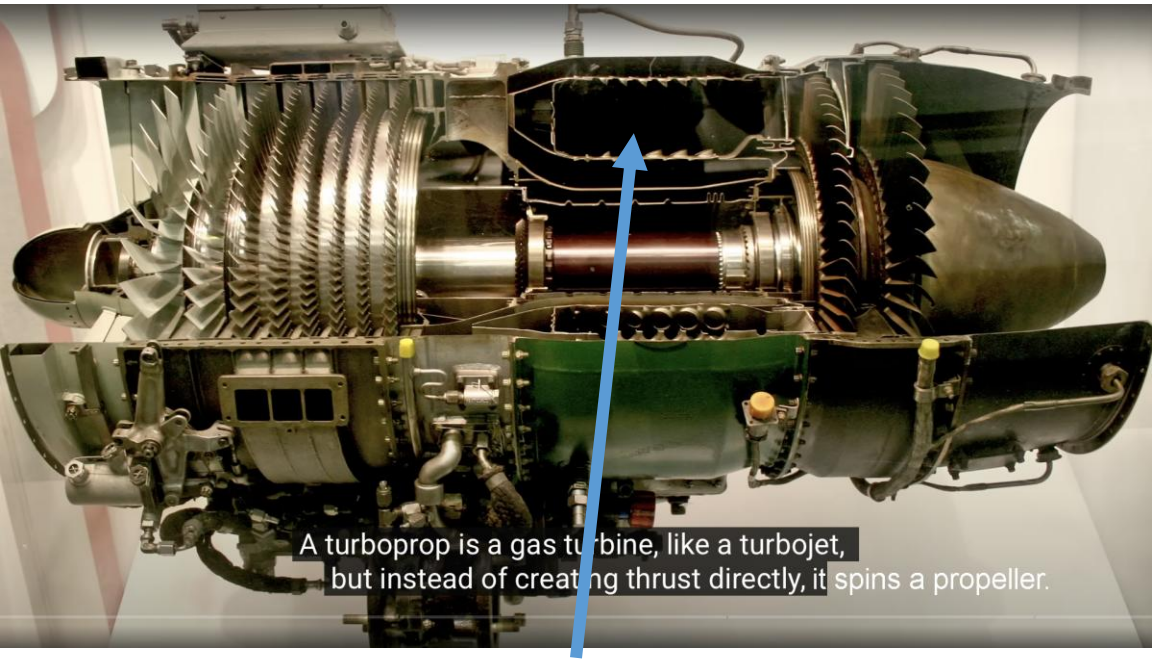
Variable VCR capability is essential for Multi-fuel operation!

➢ Ammonia & Hydrogen aviation.

- The low value of flame velocity and the needed high ignition energy of ammonia could be improved by blending it with some hydrogen (as left shown).
- Actual studies show the possibility of implementing Hydrogen bounded in Ammonia into jet propulsion systems.
- The onboard reactor (3) cracks ammonia into harmless nitrogen and water vapors.
- The classic combustion chamber (core) can be replaced by several variants of VCSR or Rotary ICEs. These provide higher torque to a significantly higher air bypass ratio for driving the propeller, e.g., in a turboprop engine.



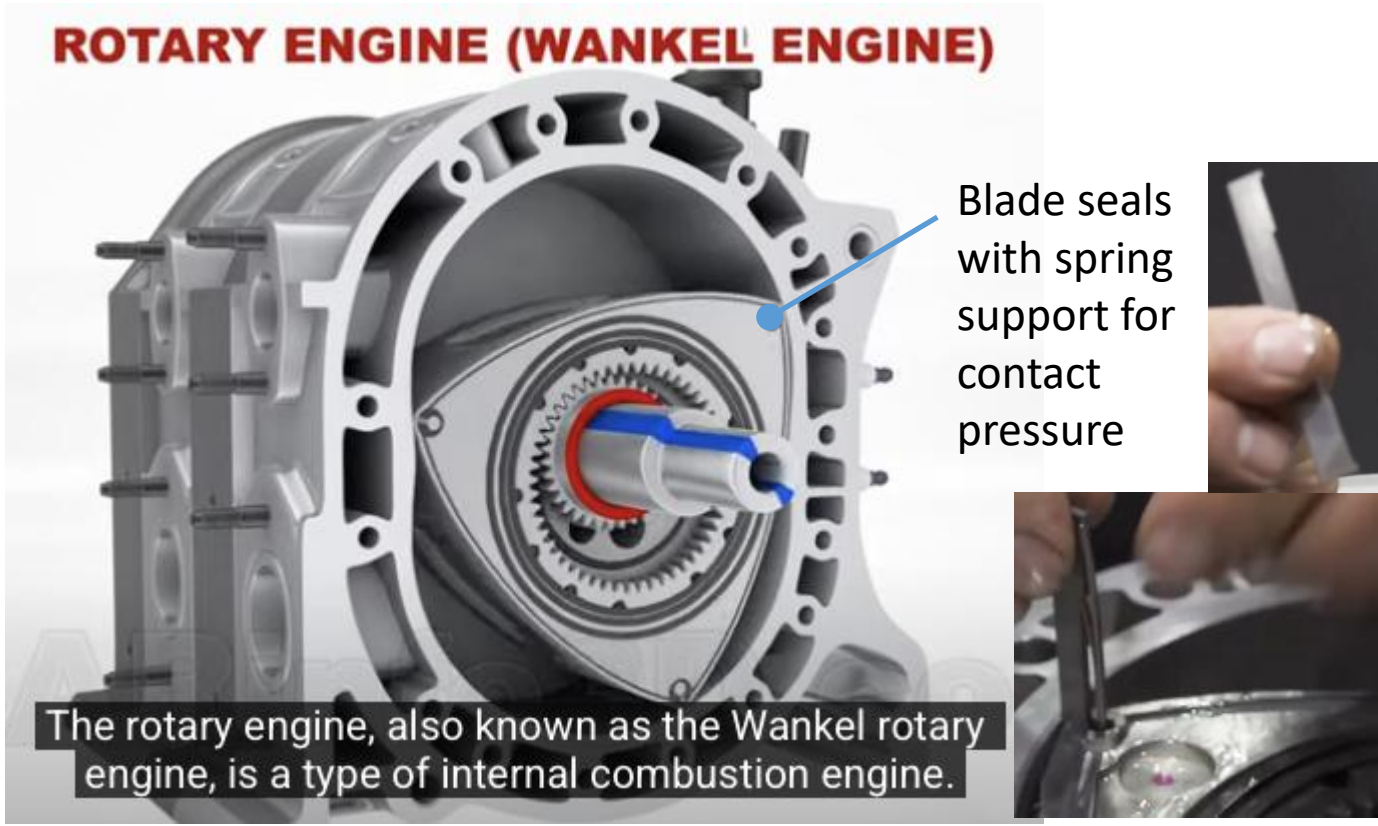
Liquid NH_3 has an LHV value 2.4 times lower than kerosene. I.e. that a 40% more efficient engine core is required for maintaining the range performances.





Instead of the usual **core** of turboprop or even turbojet engines, a reciprocating piston as VCSR or rotating piston, resp. rotary, ICE can be used.





VCSR ICE Core requirements for use in Hybrid-Electric or Turboprop Drives for Efficient, Long-Range, Multi-Fuel Propulsion.

1. Multi-Fuel Capability requires the adaptation of the Volumetric Compression ratio VCR.
2. For multi-fuel operation, the engine should have a suitable fuel supply system. Some combination as e.g. hydrogen and vaporized LPG, CNG, Methan could be operated with the same injectors as above in Multi-Fuel_Seiten aus SAE_21ICE-0132.pdf shown.
3. The increase in efficiency is achieved by using the VCSR ICE instead of the existing combustion engines. This assure at the same time the long-range capability.
4. The increase in efficiency is achieved through the implementation of True Atkinson Cycles with shorted compression and intake strokes, extended expansion and exhaust strokes, unrestrained high-pressure turbocharging and Ultra-Downsizing load control.
5. Weight, volume and specific power output of the engine are very important parameters in aviation. The VCSR 3Y engine configuration is compact, lightweight, well mass balanced and therefore produce few vibrations.

Goals pursued in the development of the new version of VCSR (named VCSR4A) ICE specifically for Aircraft applications

1. All the capabilities of the patented VCSR, presented before, should be kept in the new version VCSR4A for Aviation.
2. In addition, the design has been improved to significantly reduce the number of fixed and moving components and the force acting between them, as well as friction forces. Three patent applications will be filed in the next months:
3. The reducing of the number of fixed and moving components is the subject of the first patent application.
4. The reducing of the force between the components is the subject of the second patent application.
5. The reduction in friction forces and several other improvements are the subject of the third patent application.

Feasibility study for Hydrogen-based sustainable long-haul flights for passenger aviation based on an extreme example

Compressed Gaseous Hydrogen CGH_2-based Sustainability in Air Mobility, for large passenger aircrafts.

A simple, brief feasibility study (an estimate) using the extreme example of the **Airbus A380-800.**

The question is, to what pressure must H_2 to be compressed in the existing kerosene tanks in order to ensure equal flight performance?



Evidence chain:

1. From the available technical data:
2. The total volume V_K of all K-tanks is verified.
3. The total energy E_K of the K-fuel is calculated and used as a basis.
4. This energy E_K should be reduced for a H_2 fueled flight for at least the following reasons:
   a) The use of a new Turbofan with a modified Core, instead of the single ring combustor of Trent 970,
   b) The new Core consists of a VCSR-ICE with doubled efficiency referred to the actual one.
   c) The new Turbofan need a reduced number of stages for compressors and enable a much higher bypass ratio.
   d) This new Core enables all these while maintaining the temperature in front of the turbine.
   e) At least the reduction of the takeoff mass induced by means of H_2 fueling will be also considered.

Feasibility Estimation for a Hydrogen H_2 operation of the A380-800

$m_{empty} := 277 \cdot t$ weight

$m_{takeoff} := 575 \cdot t$ maximal

$m_{payload} := 84 \cdot t$ maximal $m_{payload.usual} := 54 \cdot t$

$m_K := 254 \cdot t$ Fuel capacity, "K" means Kerosene here, i.e. Jet A-1 fuel

Fuel situation estimation: Kerosene K versus hydrogen H_2

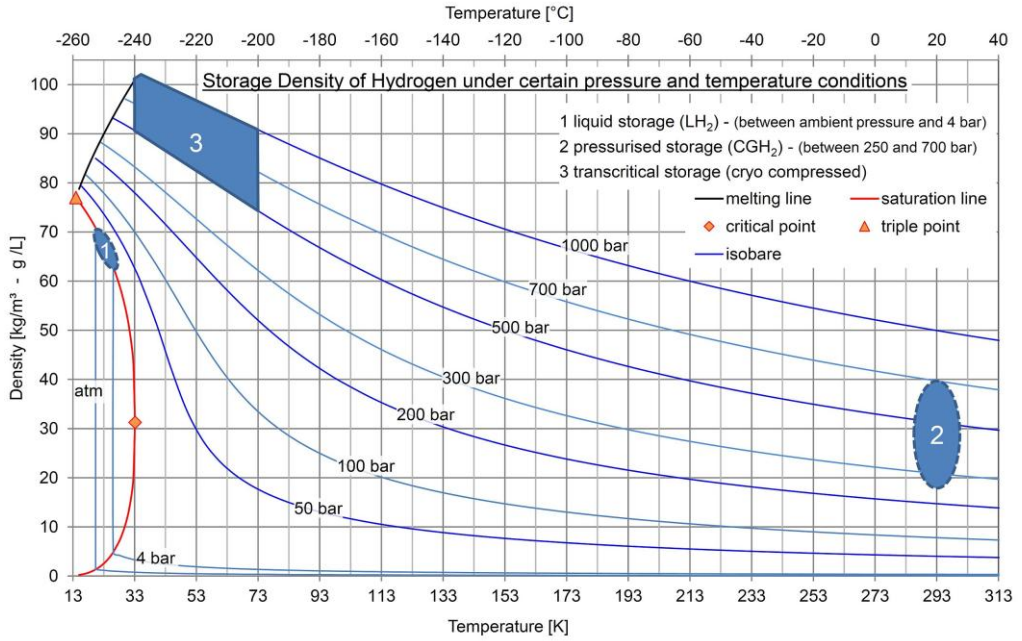
The principal question in this investigation is:

To what pressure does H_2 need to be compressed in existing K-tanks to ensure equal flight performance of the airplane?

$\rho_K := 785 \cdot \frac{kg}{m^3}$ Fuel / Kerosene density

$V_{K_tanks} := \frac{m_K}{\rho_K}$ $V_{K_tanks} = 323.6\ m^3$ existing tanks Volume

$Hu_K := 43 \cdot \frac{MJ}{kg}$ $Hu_{H2} := 120 \cdot \frac{MJ}{kg}$ lower Heating values LHV



Density-Temperature-Pressure Diagram of Hydrogen H_2

Meaning of the blue areas:

1. Liquid storage LH_2 at -250°C
2. Pressured storage CGH_2 at ambient Temperature of 20°C
3. Transcritical storage (cryogen compressed) at -220°C

Total available Energy in the actual K-fueling situation

$E_K := m_K \cdot Hu_K$ $\quad E_K = 1.09 \times 10^7 \text{ MJ}$

$\eta_{cycle.TF} := 0.25$ Efficiency of the Turbofans (TF) Trent 970 with Single annular combustor core

$\eta_{cycle.VCSR} := 0.55$ Efficiency of the Turbofans with a VCSR core,

$\eta_{bypass.TF} := 9$ Bypass Ratio of the Turbofans Trent 970 with Single annular combustor core

$\eta_{bypass.VCSR} := 25$ estimated Bypass Ratio of the Turbofans with a VCSR core

$$E_{H2needed} := E_K \cdot \frac{\eta_{cycle.TF}}{\eta_{cycle.VCSR}} \cdot \frac{\eta_{bypass.TF}}{\eta_{bypass.VCSR}} \cdot \frac{m_{takeoff} - m_K}{m_{takeoff}}$$

$$\frac{\eta_{cycle.TF}}{\eta_{cycle.VCSR}} \cdot \frac{\eta_{bypass.TF}}{\eta_{bypass.VCSR}} = 0.16 \quad \frac{m_{takeoff} - m_K}{m_{takeoff}} = 0.56$$

decreasing coefficients of the needed energy, H_2 fuel mass

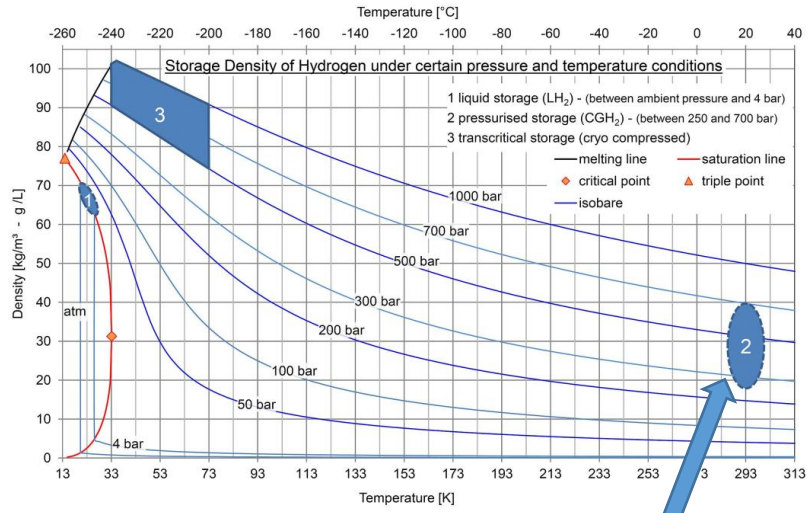
$m_{H2needed} << m_{takeoff}$, thus can be neglected here!

$$m_{H2needed} := \frac{E_{H2needed}}{Hu_{H2}} \quad m_{H2needed} = 8.3 \text{ t}$$

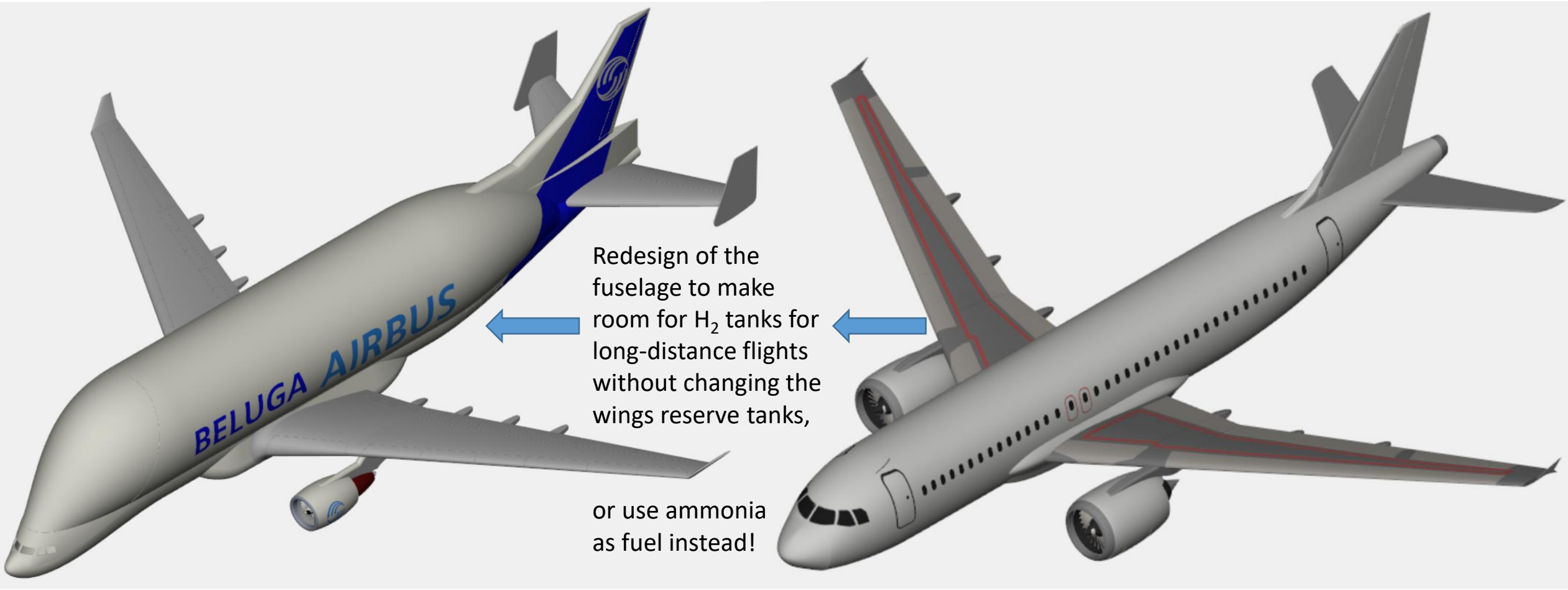
$$\frac{m_{takeoff} - m_K}{m_{takeoff} - 8.3 \cdot \text{tonne}} = 0.57$$

$$\rho_{H2needed} := \frac{m_{H2needed}}{V_{K_tanks}} \quad \rho_{H2needed} = 25.7 \frac{\text{kg}}{\text{m}^3}$$

H_2 density needed in the actual tanks



Blue area 2. CGH_2 at a pressure of 300 bar and ambient Temperature of 20°C

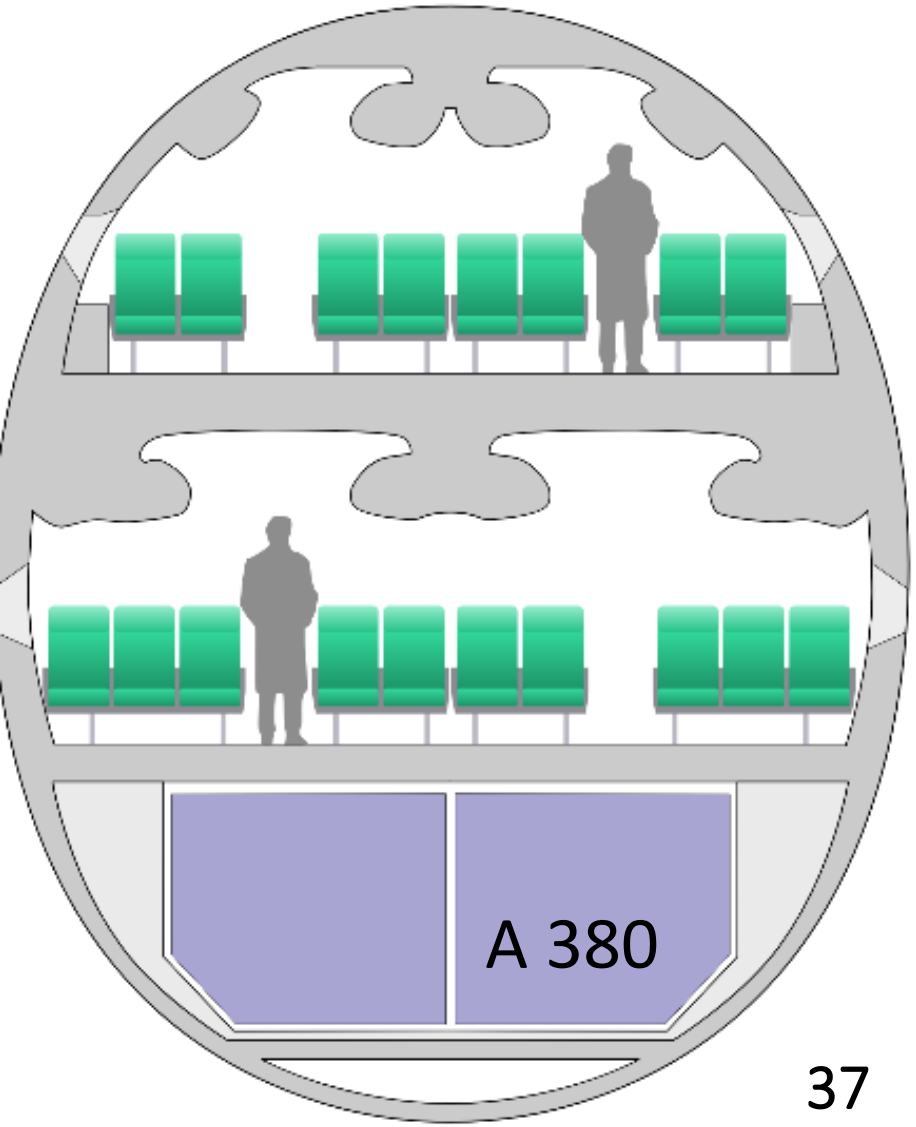


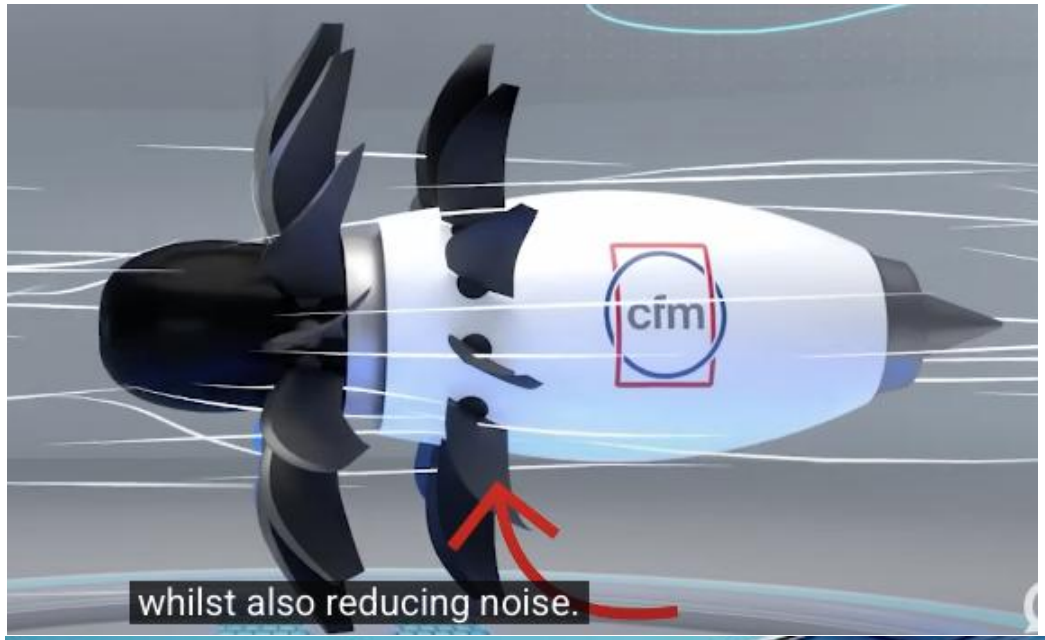
Redesign of the fuselage to make room for H_2 tanks for long-distance flights without changing the wings reserve tanks,

or use ammonia as fuel instead!

In order to use the current tanks for H_2 for operation, the pressure should be reduced to below 30 bar, which means that more volume must be available.

The upper deck can also be partially converted for H_2 tanks to enable long-range flights without changing the wings reserve tanks and fuselage design.





The original turbojet engines should be replaced by the new CFM RISE turboprop engine, but with a VCSR ICE at its Core for improved efficiency.



Feasibility Estimation for Hydrogen - Ammonia operation of the A380-800

Fuel situation estimation: Kerosene K versus Ammonia NH_3, patialy cracked in Hydrogen/Nitrogen

The principal question in this investigation is:

Which Density does Ammonia need in the existing K-tanks to ensure equal flight performance of the airplane?

$\rho_{NH3} := 626 \cdot \frac{kg}{m^3}$ at 300 bar, ambient temperature, s. Table A8-1.

$Hu_K := 43 \cdot \frac{MJ}{kg}$ $Hu_{NH3} := 18.6 \cdot \frac{MJ}{kg}$ lower Heating values

The densities of Kerosene and Ammonia are nearly the same, so no fuel mass correction is required.

$E_{NH3needed} := E_K \cdot \frac{\eta_{cycle.TF}}{\eta_{cycle.VCSR}} \cdot \frac{\eta_{bypass.TF}}{\eta_{bypass.VCSR}}$ $E_{NH3needed} = 1.8 \times 10^6 MJ$

i.e. 6 times lower as E_K

$\frac{E_K}{E_{NH3needed}} = 6.1$ $\frac{\eta_{cycle.TF}}{\eta_{cycle.VCSR}} \cdot \frac{\eta_{bypass.TF}}{\eta_{bypass.VCSR}} = 0.16$

$m_{NH3needed} := \frac{E_{NH3needed}}{Hu_{NH3}}$ $m_{NH3needed} = 96.1\,t$

$\rho_{NH3needed} := \frac{m_{NH3needed}}{V_{K_tanks}}$ $\rho_{NH3needed} = 297 \frac{kg}{m^3}$

The real density of ammonia at 300 bar & 25°C is more than twice as high as required, so that this variant is already largely feasible with lower pressure and higher temperature values if the new turbofans have a VCSR core (see the value pairs below as an example).

$\rho_{NH3_50bar_90°C} := 480 \cdot \frac{kg}{m^3}$ $\rho_{NH3_20bar_50°C} := 563 \cdot \frac{kg}{m^3}$

Table A8-1

	Energy content (LHV) [MJ/Kg]	Energy content (LHV) [MJ/L]	Density [kg/m³]	Octane [RON]	Flame-velocity [m/s]	Flammability-limits [vol/%]	Minimum Ignition Energy [mJ]
Cooled Ammonia (Liquefied)	18.6	12.69 (1 atm, -33°C)	682	>130	0.067	15-28	680
Compressed Ammonia (Liquefied)	18.6	11.65 (300 bar ,25°C)	626.	>130	0.067	15-28	680
Cooled Hydrogen (Liquefied)	120	8.5 (1atm, -253°C)	70.85	>130	3.25	4.7-75	~0.016
Compressed Hydrogen (gaseous)	120	2.46 (300 bar, 25°C)	20.54	>130	3.25	4.7-75	~0.016
Diesel (n-dodecane)	44.11	32.89 (1 atm, 25°C)	745.7[12]	<20	~0.80	0.43-0.6	~0.23
Gasoline (iso-octane)	44.34	(n-octane) 30.93 (1 atm,25°C)	(n-octane) 697.6	100	0.41 ~0.58 (RON 90-98)	0.95-6 0.6-8 (RON 90-98)	1.35 ~0.14 (RON 90-98)
Methanol	19.90	15.65 (1 atm,25°C)	786.3	108.7	0.56	6.7-36	~0.14
Ethanol	26.84	21.07 (1 atm,25°C)	785.1	108.6	0.58	3.3-19	0.6